© 2015. Published by The Company of Biologists Ltd | Journal of Cell Science (2015) 128, 1848–1861 doi:10.1242/jcs.169581

RESEARCH ARTICLE

SNX14 is a bifunctional negative regulator for neuronal 5-HT$_6$ receptor signaling

Chang Man Ha[1,2,3,*], Daehun Park[1,2,*], Yoonju Kim[1,2,4], Myeongsu Na[1,2], Surabhi Panda[5], Sehoon Won[6], Hyun Kim[7], Hoon Ryu[2], Zee Yong Park[6], Mark M. Rasenick[5] and Sunghoe Chang[1,2,4,‡]

ABSTRACT

The 5-hydroxytryptamine (5-HT, also known as serotonin) subtype 6 receptor (5-HT$_6$R, also known as HTR6) plays roles in cognition, anxiety and learning and memory disorders, yet new details concerning its regulation remain poorly understood. In this study, we found that 5-HT$_6$R directly interacted with SNX14 and that this interaction dramatically increased internalization and degradation of 5-HT$_6$R. Knockdown of endogenous SNX14 had the opposite effect. SNX14 is highly expressed in the brain and contains a putative regulator of G-protein signaling (RGS) domain. Although its RGS domain was found to be non-functional as a GTPase activator for Gαs, we found that it specifically bound to and sequestered Gαs, thus inhibiting downstream cAMP production. We further found that protein kinase A (PKA)-mediated phosphorylation of SNX14 inhibited its binding to Gαs and diverted SNX14 from Gαs binding to 5-HT$_6$R binding, thus facilitating the endocytic degradation of the receptor. Therefore, our results suggest that SNX14 is a dual endogenous negative regulator in 5-HT$_6$R-mediated signaling pathway, modulating both signaling and trafficking of 5-HT$_6$R.

KEY WORDS: SNX14, G protein-coupled receptor, Regulator of G protein signaling, Sorting nexin, Guanosine triphosphatase-activating proteins, 5-hydroxytryptamine type 6 receptor, 5-HT

INTRODUCTION

G-protein-coupled receptors (GPCRs) are seven-transmembrane domain proteins that serve to transduce the intracellular effects of a large variety of hormones or neurotransmitters subserving an equally extensive list of physiological responses (Hill, 2006). Most GPCRs couple to heterotrimeric G proteins comprised of α, β and γ subunits at the plasma membrane. In humans, there are over 20 Gα proteins encoded by 16 genes, which are subdivided into four subfamilies based on sequence identity and shared effector systems (Milligan and Kostenis, 2006). The duration of G protein signaling is controlled by the lifetime of the Gα subunit in its GTP-bound state. Although Gα subunits have intrinsic GTPase activity, auto-hydrolysis of GTP is often too slow to account for the dynamic switching of GPCR signaling (De Vries et al., 2000; Neubig and Siderovski, 2002). Proteins containing a regulator of G-protein signaling (RGS) domain bind activated Gα subunits and act as GTP-activating proteins (GAPs), accelerating GTP hydrolysis (De Vries et al., 2000). So far, RGS proteins for $G\alpha_i$, $G\alpha_q$ and $G\alpha_{12/13}$ have been well-characterized, but little is known about proteins that might regulate Gαs. Previously, SNX13 has identified been as a RGS for Gαs that is highly expressed in heart and skeletal muscle and has a role in EGFR degradation (Zheng et al., 2001).

The role of 5-hydroxytryptamine (5-HT, also known as serotonin) in cognitive processing and performance has been known for many years (Dawson, 2011). Among various 5-HT receptors, the 5-HT subtype 6 receptor (5-HT$_6$R, also known as HTR6) is one of the most recently discovered of the serotonin receptors. It is positively coupled to adenylyl cyclase and increases cAMP production upon activation. It is located almost exclusively within the central nervous system (CNS), including the striatum, olfactory tubercle, nucleus accumbens, hippocampus, cortex, cerebellum, hypothalamus and amygdala (Monsma et al., 1993; Ruat et al., 1993; Ward et al., 1995).

5-HT$_6$R is known to modulate the transmission of several neurotransmitters including acetylcholine, glutamate, dopamine, γ-aminobutyric acid, epinephrine and norepinephrine (Dawson, 2011; Mitchell and Neumaier, 2005). It is involved in various higher brain functions such as memory and cognition (Marcos et al., 2008; Mitchell et al., 2007) as well as in pathophysiological conditions such as anxiety, depression and obsessive compulsive disorder (OCD) (Svenningsson et al., 2007), Alzheimer's disease (Geldenhuys and Van der Schyf, 2008), drug addiction (Lecca et al., 2004) and schizophrenia (Masellis et al., 2001). Recent evidence also suggests it has a role in obesity (Heal et al., 2011). Over the past decade, 5-HT$_6$R has gained increasing attention and its antagonism has become a promising target for the treatment of various neuropsychological diseases. Nevertheless, very little is known about its regulation and function in the brain.

SNX14 is a member of the sorting nexin family, predicted to have for roles in protein sorting and vesicular trafficking (Carlton et al., 2005). It contains a putative RGS domain and a phox homology (PX) domain, an N-terminal hydrophobic region and a PX-associated (PXA) domain (Worby and Dixon, 2002). SNX14 has been isolated from mouse embryonic stem cell (ESC)-derived neurons and was found to be expressed at high levels in the nervous system (Carroll et al., 2001). A recent study has found that SNX14 protein levels are progressively increased during neuronal development, whereas its knockdown severely impairs

[1]Department of Physiology and Biomedical Sciences, Seoul National University College of Medicine, Seoul 110-799, South Korea. [2]Biomembrane Plasticity Research Center, Seoul National University College of Medicine, Seoul 110-799, South Korea. [3]Department of Structure and Function of Neural Network, Korea Brain Research Institute, Daegu 700-100, South Korea. [4]Neuroscience Institute, Seoul National University College of Medicine, Seoul 110-799, South Korea. [5]Departments of Physiology & Biophysics and Psychiatry, University of Illinois at Chicago, Jesse Brown VA Medical Center, Chicago, IL 60680, USA. [6]Department of Life Science, Gwangju Institute of Science and Technology, Gwangju 500-712, South Korea. [7]Department of Anatomy, Korea University College of Medicine, Seoul 136-705, South Korea.
*These authors contributed equally to this work

‡Author for correspondence (sunghoe@snu.ac.kr)

Received 1 February 2015; Accepted 13 March 2015

both excitatory and inhibitory synaptic transmission (Huang et al., 2014). Another study has found that SNX14 mutations cause a distinctive autosomal-recessive cerebellar ataxia and intellectual disability syndrome (Thomas et al., 2014). Therefore, these results suggest that there is an essential role for SNX14 in neuronal development and function, but the underlying mechanism(s) for this remain poorly understood.

Here, we provide evidence that SNX14 is highly expressed in the brain, and as a sorting nexin, it interacts with 5-HT_6R and accelerates internalization and degradation of 5-HT_6R. Knockdown of endogenous SNX14 prolonged the cell surface expression of 5-HT_6R. Although we found that the SNX14 RGS domain does not retain GAP activity for Gαs, it specifically bound to and sequestered Gαs, thus inhibiting the 5-HT_6R-mediated signaling pathway. We further reveal that the binding affinity of SNX14 for Gαs was almost abolished by phosphorylation of RGS domain by protein kinase A (PKA) and that phosphorylation of SNX14 is also required for the endocytic degradation of 5-HT_6R. Taken together, our results suggest that SNX14 is a dual negative regulator in 5-HT_6R-mediated signaling pathways that acts by both sequestering Gαs and inducing endocytosis of 5-HT_6R.

RESULTS

SNX14 associates with 5-HT_6R

SNX14 consists of a putative RGS domain, a PX domain, an N-terminal hydrophobic region and a PXA domain (Fig. 1A; supplementary material Fig. S1A). *In situ* hybridization showed that SNX14 was highly expressed in the hippocampus, nucleus accumbens and cerebellum (Fig. 1B), where 5-HT_6R is also abundantly expressed. Immunoblotting also showed that SNX14 was also highly expressed in lung, testis and brain regions, such as the hippocampus, cerebellum and cerebral cortex, but that virtually no expression was observed in heart and muscle where SNX13 is known to be abundant (Zheng et al., 2001), suggesting a mutually exclusive tissue distribution (Fig. 1C). High levels of SNX14 expression were also detected in primary hippocampal neurons, glial cells and in the HT-22 hippocampal cell line but not in HEK293T, HeLa or COS-7 cells (Fig. 1D; supplementary material Fig. S1B).

Previous studies have shown that SNX3 regulates endosomal trafficking through its PX-domain-mediated interaction with PtdIns(3)*P* (Xu et al., 2001). Examination of the phosphoinositide-binding behavior of SNX14 showed that the PX domain bound both PtdIns(3)*P* and PtdIns(5)*P*, whereas the PXA domain bound PtdIns(3,4)P_2, PtdIns(3,4,5)P_3 and PtdIns(4,5)P_2. Full-length SNX14 displayed a combination of the lipid binding patterns of the PX and PXA domains. Accordingly, the heterogeneously expressed SNX14 domain mutants localize in endosome-like structures in the cytosol or at the plasma membrane, suggesting that SNX14 might play a role in membrane trafficking (supplementary material Fig. S1C,D).

5-HT_6R is a Gαs-linked serotonin receptor and SNX14 contains a putative RGS domain. The closely related protein SNX13 has been reported to act as an RGS for Gαs. Given that the expression profiles in the CNS are similar for SNX14 and 5-HT_6R, we wondered whether SNX14 interacts with 5-HT_6R. The third intracellular loop (iL3) has a fairly long stretch of amino acids and a previous study has shown that iL3 of 5-HT_6R interacts with Gαs (Kang et al., 2005). Micro-liquid chromatography tandem mass spectrometry (LC-MS/MS) analysis using immunoprecipitated brain lysates with GST-conjugated iL3 of 5-HT_6R showed that besides various endocytic proteins, such as dynamin, AP-2, amphiphysin and epsin, SNX14 was also identified as one of its endogenous binding partners (Fig. 1E).

When heterogeneously expressed in COS-7 cells, 5-HT_6R interacted with the full-length SNX14 and RGS-PX domain of SNX14 but not with SNX9 and SNX18 (Fig. 1F). We determined that the interaction between 5-HT_6R and SNX14 was mediated by the iL3 of 5-HT_6R and the RGS domain of SNX14 (Fig. 1G). The K262 and K265 residues of iL3 appear to be the binding sites for SNX14 because a K262A and K265A double mutant showed little interaction with SNX14 (Fig. 1H). The RGS of SNX14 did not interact with β_2 adrenergic receptor (β_2AR, also known as ADRB2) or dopamine D_1 receptor (D_1DR, also known as DRD1), which are related Gαs-linked GPCRs (Fig. 1I).

SNX14 accelerates internalization and degradation of the 5-HT_6R

Next, we tested whether the interaction between SNX14 and 5-HT_6R plays a role in endocytic trafficking of 5-HT_6R. The RGS-PX domain of SNX14 was coexpressed with 5-HT_6R in HEK293T cells and cells were treated with 5-HT to induce internalization of 5-HT_6R. Curiously, the expression of the RGS-PX domain decreased total and surface 5-HT_6R to the same extent seen in control cells after 30 min exposure to 5-HT. Treatment of these cells with 5-HT evoked no further decrement of total or surface 5-HT_6R (Fig. 2A–D). This endocytic degradation by the RGS-PX domain was not detected for β_2AR (Fig. 2B–D).

These results suggest that SNX14 dramatically increases the rate of constitutive endocytosis and degradation of 5-HT_6R. This is confirmed by experiments using Tet-On inducible expression of the RGS-PX domain in cells transiently or stably expressing 5-HT_6R (Fig. 2E). Using liposome-mediated delivery of purified the RGS-PX domain of SNX14, we show that 5-HT_6R gradually decreased from the cell surface after delivery of purified the RGS-PX domain (Fig. 2F). We found that not only the RGS-PX domain but also full-length SNX14 had a similar effect and further found that phosphoinositide-binding property of the PX domain is required given that the ΔPX mutant of SNX14 failed to induce 5-HT_6R internalization (Fig. 3A–E). Endogenous SNX14 was recruited to the plasma membrane by 5-HT treatment in HT-22 cells (supplementary material Fig. S2A). Total internal reflection fluorescence (TIRF) imaging also demonstrated that full-length SNX14 was recruited to the plasma membrane by 5-HT treatment and that some of SNX14 spots were re-internalized (Fig. 3F–J).

Knockdown of SNX14 expression prolongs the expression of 5-HT_6R

We next investigated whether knockdown of SNX14 alters the expression of 5-HT_6R in HT-22 cells that endogenously express high levels of SNX14 and 5-HT_6R. Three independent short hairpin RNA (shRNA) constructs targeting SNX14 were made (Fig. 4A) and suppression of SNX14 expression by shRNA1 and shRNA2 in HT-22 cells was confirmed, whereas shRNA3 had no effect (Fig. 4B). When endogenous expression of SNX14 was suppressed by shRNA1, shRNA2 or shRNA1+2, the levels of 5-HT_6R were significantly higher than those in the control or shRNA3-transfected cells (Fig. 4B). Furthermore, 5-HT exposure did not further downregulate 5-HT_6R in shRNA1+2-transfected cells, supporting the conclusion that SNX14 accelerates endocytosis of 5-HT_6R (Fig. 4C–E). The levels of SNX14 stayed relatively constant over time after 5-HT treatment even in the presence of phosphatase (Fig. 4F,G).

Journal of Cell Science (2015) 128, 1848–1861 doi:10.1242/jcs.169581

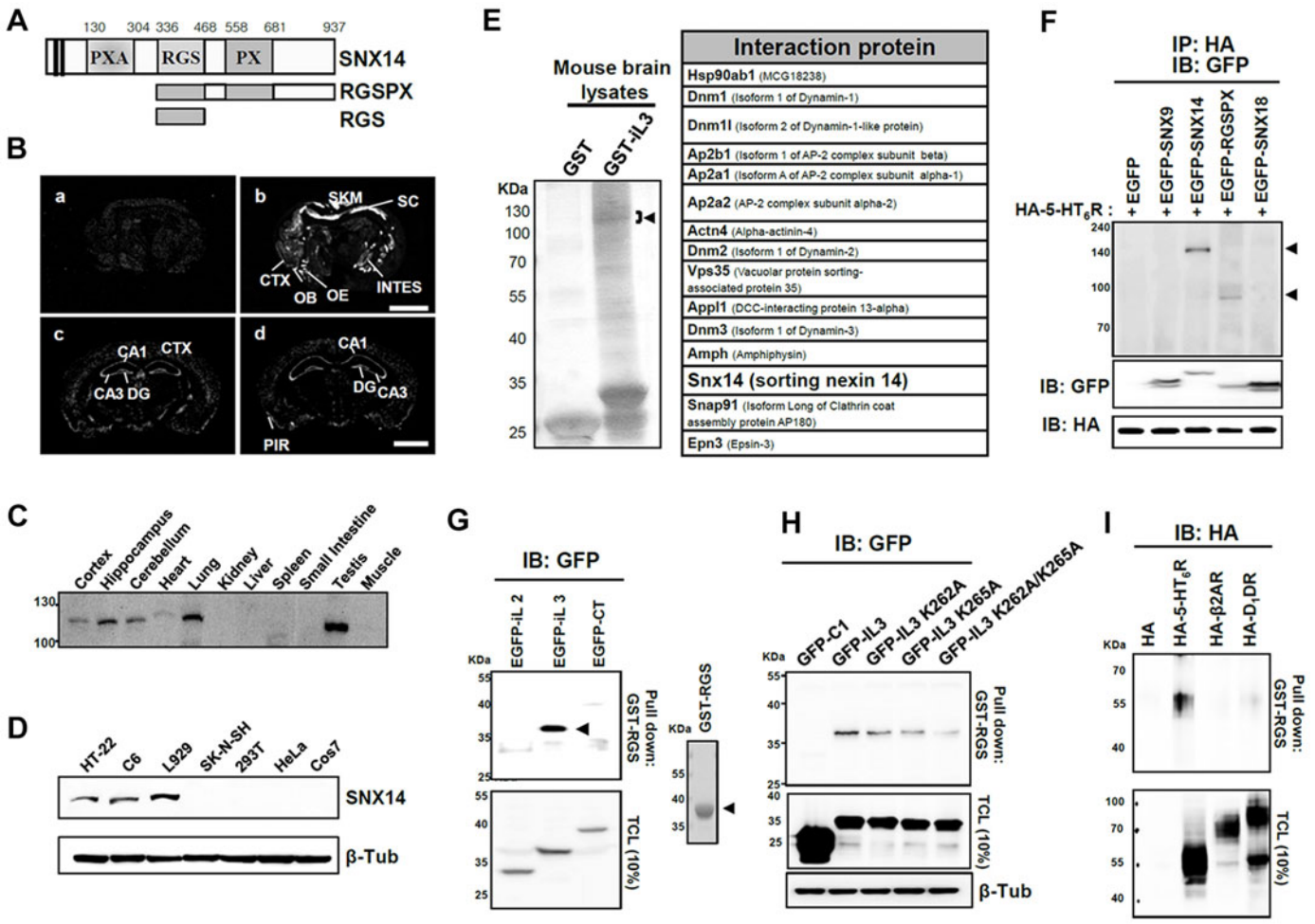

Fig. 1. SNX14 associates with 5-HT$_6$R. (A) Schematic representation of full-length, the RGS-PX domain (RGSPX) and RGS domains of SNX14 used in the study. There are two putative transmembrane domains at the N-terminus (black bars). (B) Localization of SNX14 mRNA as visualized by *in situ* hybridization. Shown are negative film images of *in situ* hybridization of parasagittal sections from E16 (a) and E18 (b) embryos and coronal sections from P21 (c) and adult (d) rat brain. CTX, cortex; CA1, hippocampal CA1 area; INTES, intestine; OB, olfactory bulb; OE, olfactory epithelium; PIR, piriform cortex; SKM, skeletal muscle; SC, spinal cord. Scale bars: 6 mm in sagittal sectioned embryo; 3 mm in coronal sectioned brain. (C) Tissue distribution of SNX14 protein in >4-week-old C57BL/6 mice as assessed with an anti-SNX14 antibody. (D) Endogenous SNX14 is expressed in brain lineage cell lines. Cell lines: HT-22, mouse hippocampal; C6, rat glioma; L929, mouse fibrosarcoma; SK-N-SH, human neuroblastoma; HEK293T, human embryonic kidney; HeLa, human cervical cancer; COS-7, African green monkey kidney fibroblast. (E) SNX14 interacts with 5-HT$_6$R. Mouse brain lysates were incubated at 4˚C for 2 h with purified GST or GST–iL3 of 5-HT$_6$R bound to glutathione beads in a lysis buffer, separated by SDS-PAGE and silver-stained. The band indicated by the arrowhead was excised and analyzed by micro-LC-MS/MS. We performed micro-LC-MS/MS analysis twice and the listed proteins were identified in both trials. (F) HEK293T cells were co-transfected with 3×HA–5-HT$_6$R and EGFP, EGFP–SNX14, the EGFP-tagged RGS-PX domain of SNX14 (EGFP–RGSPX, amino acids 336–937), EGFP–SNX9 or EGFP–SNX18. Lysates were immunoprecipitated (IP) with anti-HA antibody and immunoblotted (IB) with anti-GFP antibody. The arrowheads indicate the size of EGFP–SNX14 (137 kDa) and EGFP–RGSPX (93 kDa). (G) HEK293T cells were transfected with EGFP-tagged iL2, iL3 and the C-terminal (CT) of 5-HT$_6$R, lysed and pulled down with a purified SNX14 GST-tagged RGS domain (GST–RGS, 15 μg). Residual cell lysates (10% of total cell lysates; TCL) were subjected to SDS-PAGE and immunoblotted with anti-GFP antibody. The RGS domain of SNX14 specifically interacts with the iL3 domain of 5-HT$_6$R. (H) HEK293T cells were transfected with GFP, GFP–iL3 and GFP–iL3 mutants (K262A, K265A or K262A/265A), lysed and pulled down with purified GST–RGS. The immunoprecipitated proteins were immunoblotted with anti-GFP antibody. (I) HEK293T cells were transfected with HA, 3×HA–5-HT$_6$R, HA–β_2AR or HA–D_1DR, lysed and pulled down with purified GST–RGS. The same amount of GST–RGS (shown in the Coomassie staining in G) was used in G, H and I for the pulldown assay.

SNX14 does not retain GAP activity but specifically binds and sequesters Gαs, thus inhibiting 5-HT$_6$R downstream signaling pathway

SNX14 contains a putative RGS domain (Fig. 1A; supplementary material Fig. S1A). Given that the closely related protein, SNX13 has been reported to act as a RGS for Gαs (Zheng et al., 2001), we evaluated whether SNX14 also acts as a RGS-GAP for Gαs. We found that SNX14 bound to the activated form of Gαs [activation was achieved by addition of aluminium magnesium fluoride (AMF), GTPγs or the Q227L mutation, each of which promotes conformational changes that resemble the transition state of Gαs (Tesmer et al., 1997)]. SNX14 did not bind to wild-type Gαi1 or the active form of Gαi1 (Q204L) even in the presence of AMF. The isolated RGS domain of SNX14 interacted with constitutively active Gαs (Q227L) and with wild-type Gαs but not with wild-type Gαi1 or the active form of Gαi1 (Q204L) (Fig. 5A). SNX14 or activated Gαs was, respectively, pulled down with GST–Gαs or the GST–RGS domain from mouse brain

Journal of Cell Science (2015) 128, 1848–1861 doi:10.1242/jcs.169581

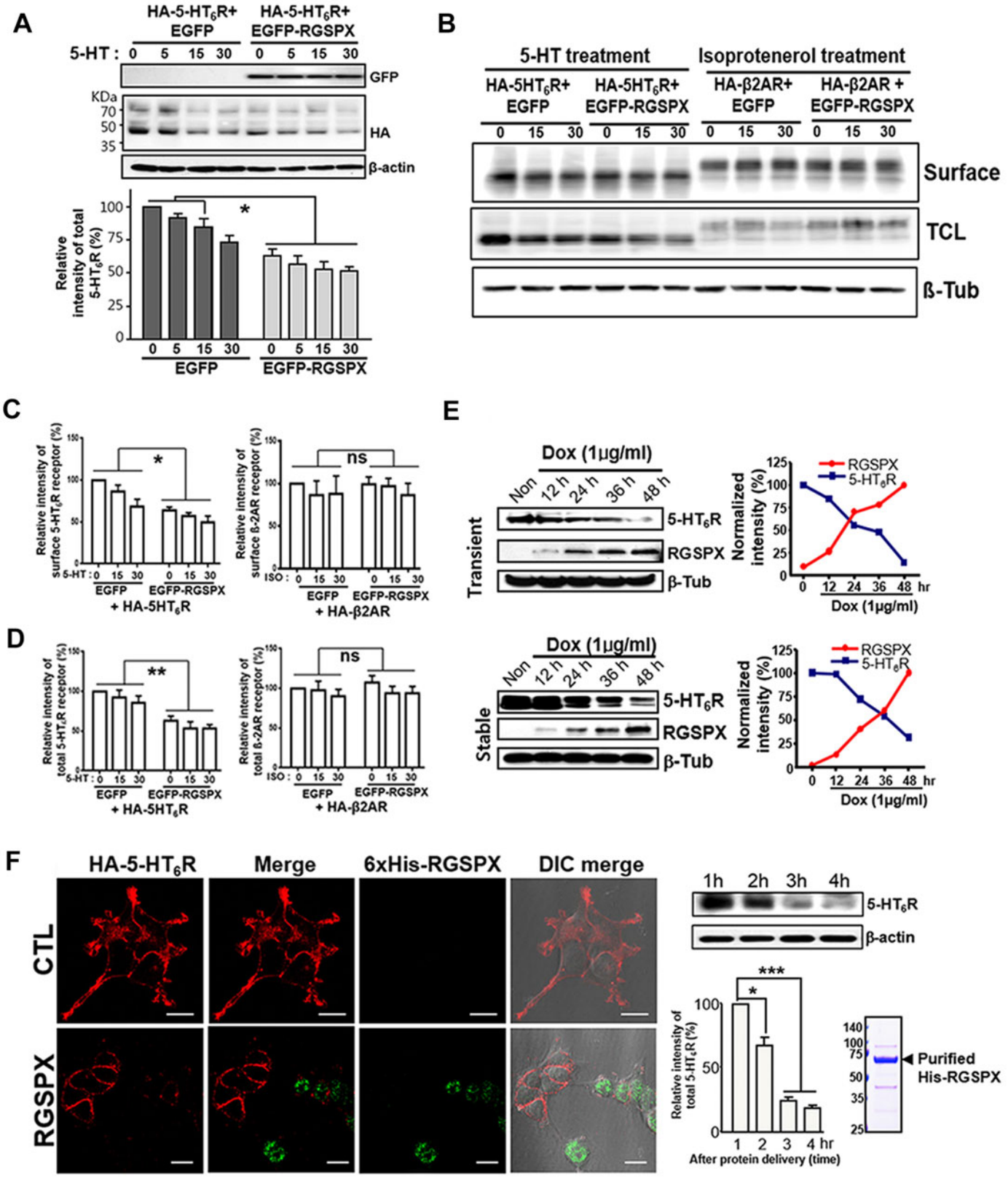

Fig. 2. See next page for legend.

lysates (Fig. 5B). In addition, purified His–Gαs (AMF-activated) interacted with the purified GST–RGS domain but not with GST–RGS4 (Fig. 5C). Mutationally activated Gαs (Q227L) also strongly bound to the purified GST–RGS domain but not to GST–RGS4 (Fig. 5C), suggesting that there is a specific interaction between the RGS domain of SNX14 and Gαs. We

Fig. 2. SNX14 accelerates internalization and degradation of the 5-HT$_6$R. (A) HEK293T cells were co-transfected with 3×HA–5-HT$_6$R and EGFP or the EGFP-tagged RGS-PX domain of SNX14 (EGFP–RGSPX). After 5-HT treatment for the times indicated, the cells were lysed and immunoblotted with anti-GFP, anti-HA or anti-β-actin antibody. Data were normalized to the initial level of 5-HT$_6$R in the EGFP control and are presented as means±s.e.m. (n=6). *P<0.05 between EGFP control and the RGS-PX domain at each time point (ANOVA and Tukey's HSD post hoc test). (B–D) HEK293T cells were co-transfected with HA-5-HT6R or HA-β2AR and EGFP-C1 or EGFP–RGSPX. 48 h after transfection, the cells were starved for 16 h and treated with 10 μM 5-HT or 25 μM isoproterenol (Iso) for the times indicated. Surface biotinylation was performed and surface and total proteins were identified with anti-HA antibody. The levels of surface (C) and total (D) proteins were normalized to the level at 0 min of each receptor in the EGFP control and are presented as means±s.e.m. (n=3). *, P<0.05 (ANOVA and Tukey's HSD post hoc test); ns, not significant. (E) Coordination of the RGS-PX domain expression and 5-HT$_6$R loss. HEK293 cells expressing 5-HT$_6$R were transiently or stably transfected with the RGS-PX domain using the Tet-On system. Cells were cultured with or without 1 μg/ml doxycycline (Dox). The intensity values of 5-HT$_6$R at the indicated times were normalized to that at time zero and the intensity values of the RGS-PX domain at the times indicated were normalized to that at time 48 h to emphasize the internalization of surface 5-HT$_6$R. The expression of the RGS-PX domain and the internalization of 5-HT$_6$R are tightly correlated after Dox treatment. (F) Introduction of the RGS-PX domain reduces the levels of 5-HT$_6$R. A 6×His-tagged RGS-PX protein (6×His–RGSPX) was purified as described in the Materials and Methods (see gel on the right). HEK293 cells stably expressing 5-HT$_6$R were transfected purified 6×His–RGSPX protein using the Chariot™ system. Cells were incubated with Chariot complex for 2 h, then fixed and stained with Alexa-Fluor-594-conjugated anti-rat antibody for 3×HA–5-HT$_6$R and Alexa-Fluor-488-conjugated anti-mouse antibody for the 6×His-RGSPX (left panel). Scale bars: 20 μm. The cells were lysed at the times indicated after protein delivery and immunoblotted with anti-HA-antibody. Lower bar graph: the quantification from three independent experiments. Data are mean±s.e.m. *P<0.05, ***P<0.001 (ANOVA and Tukey's HSD post hoc test).

next investigated whether SNX14 could potentiate the GTPase activity of Gαs. GTP single-turnover assays showed that SNX14 did not promote the GTPase activity of Gαs (Fig. 5D).

Given that SNX14 does not possess GAP activity for Gαs, we queried the physiological meaning of the SNX14–Gαs interaction by performing cAMP production assays. 5-HT increased cellular cAMP in control cells but not in cells expressing the RGS domain of SNX14. cAMP elevation in the presence of forskolin, which activates Gαs in the absence of adenylyl cyclase, was equivalent in the presence or absence of SNX14 (Fig. 5E). These results suggest that SNX14 acts as a negative regulator that inhibits Gαs-mediated cAMP production perhaps by binding and sequestering Gαs. We found that endogenous SNX14 was located in endosome-like punctate structure, but upon addition of 5-HT, SNX14 translocated to the plasma membrane (supplementary material Fig. S2B,C). TIRF imaging also showed that SNX14 appeared to be recruited to the plasma membrane by 5-HT treatment coincidently with Gαs, and they disappeared together (supplementary material Fig. S2C).

The iL3 region of 5-HT$_6$R is known to directly bind to Gαs (Kang et al., 2005). Given that we found that the RGS of SNX14 also interacts with iL3 of 5-HT$_6$R (Fig. 1G,H), we tested whether the RGS of SNX14 and Gαs competitively bind to iL3 of 5-HT$_6$R. The interaction between RGS of SNX14 and iL3 of 5-HT$_6$R gradually decreased, with a concomitant increase in the interaction between Gαs and iL3 of 5-HT$_6$R upon increasing the amount of Gαs protein in the reaction (Fig. 6A–D), suggesting that there is a competition between RGS of SNX14 and Gαs in their binding to iL3 of 5-HT$_6$R.

PKA-mediated phosphorylation of SNX14 re-routes SNX14 from Gαs binding to 5-HT$_6$R binding, facilitating the internalization of that receptor

We next tested whether SNX14 is phosphorylated by cAMP-dependent PKA, a downstream effector of Gαs-mediated signaling pathways. Indeed, SNX14 was phosphorylated at serine and threonine, but not tyrosine residues, upon forskolin treatment (Fig. 7A–C). We found that recombinant RGS was strongly phosphorylated *in vitro* by the catalytic subunit of PKA (PKAnes) (Fig. 7D) and LC-MS/MS showed that the RGS domain was phosphorylated on S382 and S388 (supplementary material Fig. S3). Although these serine residues are not canonical sites for PKA phosphorylation, PKA-mediated phosphorylation was markedly reduced in an S382A/S388A double mutant of RGS (supplementary material Fig. S3; Fig. 7D). This was further confirmed in cells transfected with RGS or various S382/S388 mutants and PKAnes. The phosphorylation of RGS increased by PKAnes was substantially reduced in S382A/S388A single or double mutants (Fig. 7E).

We next tested whether phosphorylation of SNX14 affects its binding to Gαs. Firstly, when transfected with PKAnes, there was dramatic reduction in the interaction between the RGS-PX domain of SNX14 and Gαs in the presence of AMF or a constitutively active Gαs (Q227L) (Fig. 7F). Secondly, the single or double phospho-mimetic mutants (S382D/S388D) of RGS either markedly reduced or completely abolished the binding between RGS and Gαs (Fig. 7G). These results suggest that the phosphorylation of RGS domain by PKA dramatically decreases its affinity for Gαs.

We next tested whether phosphorylation affects the SNX14-induced endocytic trafficking of surface 5-HT$_6$R. Interestingly, the S382A/S388A double phospho-deficient mutant did not promote endocytosis of 5-HT$_6$R whereas the S382D/S388D double phospho-mimetic mutant had an effect on 5-HT$_6$R levels similar to the RGS-PX domain (Fig. 8A,B). These results suggest that PKA-mediated phosphorylation of SNX14 is required for its effect on internalization of 5-HT$_6$R. We tested further this possibility using the PKA inhibitor, H-89. After H-89 treatment, co-expression of the RGS-PX domain did not decrease the initial levels of either total or surface levels of 5-HT$_6$R (Fig. 8C–F). Given that we showed that phosphorylated the RGS-PX domain no longer binds Gαs (Fig. 7F,G), our results imply that phosphorylated SNX14 might be 're-routed' for preferential binding to 5-HT$_6$R, thus enhancing endocytic internalization and degradation of that receptor.

DISCUSSION

In this study, we found that SNX14, as might be expected of a sorting nexin, accelerates internalization and degradation of 5-HT$_6$R. We also found that SNX14 specifically binds and sequesters Gαs, thus inhibiting downstream cAMP production. We, thus, provide strong evidence that SNX14 plays roles as an endogenous negative regulator of 5-HT$_6$R trafficking and signaling.

Besides Gαs, 5-HT$_6$R is known to interact with various proteins such as Fyn tyrosine kinase (Yun et al., 2007), Jun activation domain-binding protein-1 (Jab1, also known as COPS5) (Yun et al., 2010), mammalian target of rapamycin (mTOR) (Meffre et al., 2012), microtubule-associated protein 1B light chain (MAP1B-LC) (Kim et al., 2014) and cyclin-dependent kinase 5 (Cdk5) (Duhr et al., 2014). The C-terminus of 5-HT$_6$R interacts with the Fyn and activation of 5-HT$_6$R stimulates

Journal of Cell Science (2015) 128, 1848–1861 doi:10.1242/jcs.169581

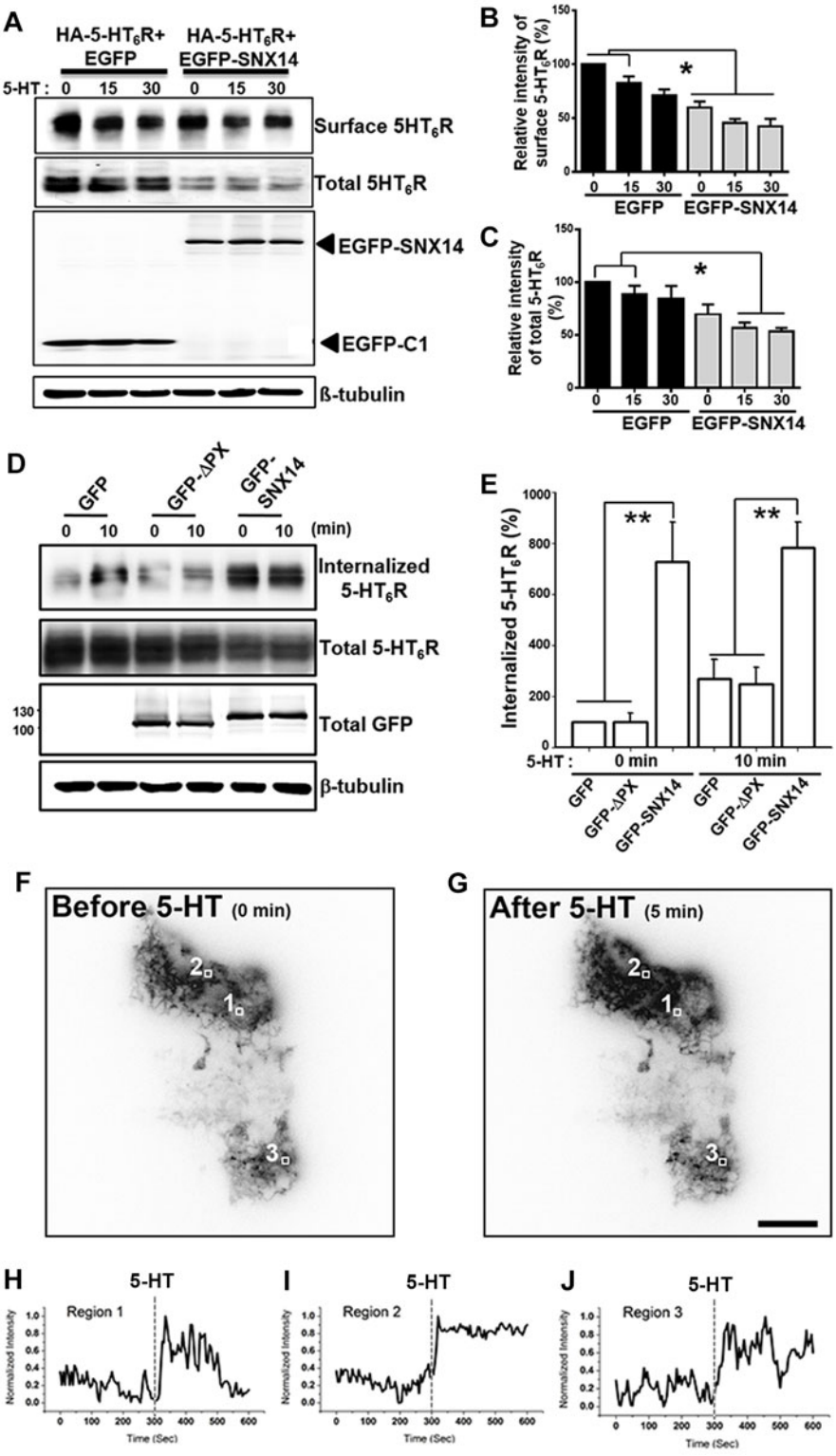

Fig. 3. The full-length SNX14 accelerates internalization and degradation of the 5-HT$_6$R and shuttles between the plasma membrane and the cytosol. (A) 3×HA–5-HT$_6$R stable HEK293 cells were transfected with EGFP-C1 (control) or EGFP–SNX14. 48 h after transfection, the cells were starved for 16 h and treated with 10 μM 5-HT for the times indicated, followed by immunoblotting with anti-GFP, anti-HA or anti-β-tubulin antibody. Surface biotinylation was performed to detect the internalization of 5-HT$_6$R. (B,C) Data were normalized to the level at 0 min of 5-HT$_6$R in the EGFP control and are presented as means±s.e.m. *P<0.05 from three independent experiments (ANOVA and Tukey's HSD post hoc test). (D) The PX domain of SNX14 is required for the internalization of 5-HT$_6$R. 5-HT$_6$R stable cells were transfected with GFP empty vector, a GFP-tagged PX deletion mutant (GFP–ΔPX) and GFP–SNX14. After surface biotinylation, cells were treated with 5-HT for the times indicated and internalized 5-HT$_6$R was detected by western blotting. (E) The internalized 5-HT$_6$R levels were normalized to those at 0 min in the EGFP control. Data are presented as means±s.e.m. from three independent experiments. **P<0.001 (ANOVA and Tukey's HSD post hoc test). (F,G) TIRF microscope images of EGFP–SNX14 full-length trafficking in 5-HT$_6$R stable cells transiently expressing with EGFP–SNX14. Time-lapse series images were collected for 5 min at 37°C in the absence or presence of 10 μM 5-HT. Each still image corresponds to a frame acquired before (F) and 5 min after 5-HT treatment (G). (H–J) Normalized fluorescence intensity changes as a function of time of three representative EGFP–SNX14 spots. EGFP–SNX14 spots selected from time series show three different behaviors. Region 1: a spot was rapidly recruited to the surface, stayed and disappeared (H). Region 2: a spot stayed on the surface during the entire acquisition time (I). Region 3: a spot was recruited to the surface, remained, disappeared and reappeared (J).

extracellular-regulated kinase 1/2 through the Fyn-dependent pathway (Yun et al., 2007). 5-HT$_6$R also interacts with mTORC1 and activates the phosphoinositide 3-kinase (PI3K), Akt and mTOR signaling pathway in prefrontal cortex, and recruitment of mTOR by 5-HT$_6$R contributes to the perturbed cognition in schizophrenia (Meffre et al., 2012). In addition, the C-terminus and iL3 of 5-HT$_6$R selectively interact with the N-terminus and C-terminus of Jab1, respectively. Interestingly, hypoxia increases the expression level of 5-HT$_6$R and Jab1, indicating that 5-HT$_6$R and the Jab1 complex and its downstream signaling pathway protect the cells against hypoxia (Yun et al., 2010). A recent study has further shown that direct recruitment of CDK5 and p35 (also known as CDK5R1) to the C-terminus of 5-HT$_6$R leads to the phosphorylation of this region and promotes neurite outgrowth by activating Cdc42 (Duhr et al., 2014). Such diverse 5-HT$_6$R-mediated downstream signaling pathways and

Journal of Cell Science (2015) 128, 1848–1861 doi:10.1242/jcs.169581

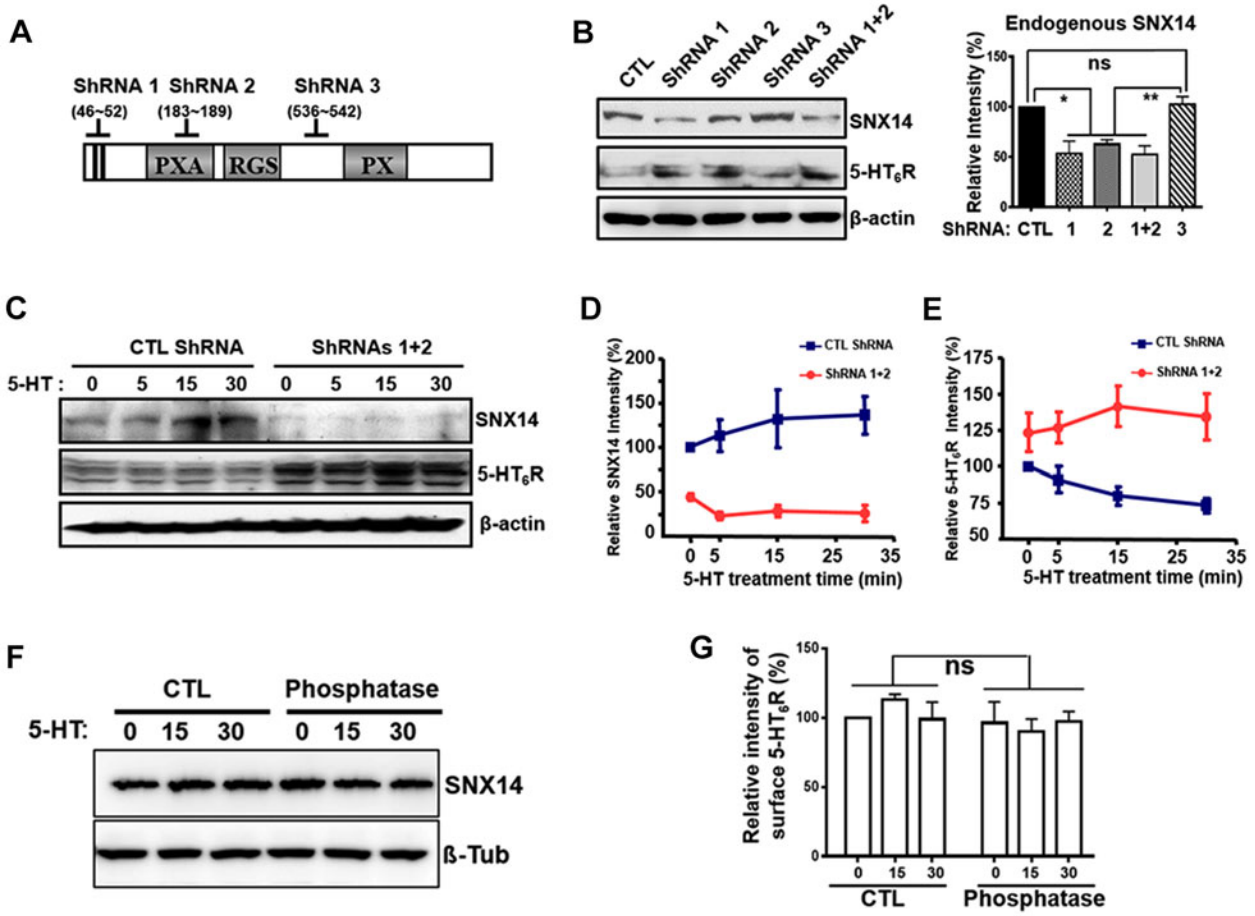

Fig. 4. Knockdown of SNX14 expression prolongs the expression of 5-HT$_6$R. (A) Schematic representation of shRNA targeting sites on SNX14. (B) Inverse correlation of the expression of SNX14 and 5-HT$_6$R. HT-22 cells that endogenously express both SNX14 and 5-HT$_6$R were transfected with pU6-mRFP (CTL) or the indicated shRNAs. After 48 h transfection, the cells were lysed and immunoblotted with anti-SNX14, anti-5-HT$_6$R or anti-β-actin antibody. Quantification of endogenous SNX14 levels from four independent experiments. Data represented the relative intensity to the levels of SNX14 in the control (CTL). *P<0.05; **P<0.01; ns, not significant (ANOVA and Tukey's HSD post hoc test). (C) After 48 h transfection, HT-22 cells were treated with 10 μM 5-HT for the times indicated, lysed and analyzed by immunoblotting with antibodies against SNX14, 5-HT$_6$R and β-actin, respectively. (D,E) Quantification of endogenous levels of SNX14 and 5-HT$_6$R at the indicated times after 5-HT treatment from four independent experiments. Data represent the relative intensity of each protein to that of the control at the time 0. (F,G) The levels of SNX14 stayed relatively constant over the time after 5-HT treatment. HT-22 cells were treated with 5-HT for the indicated times, lysed and incubated with or without 2 unit/ml of phosphatase. Data were normalized to the initial level of SNX14 in the EGFP control and are presented as means±s.e.m. from three independent experiments. ns, not significant (ANOVA and Tukey's HSD post hoc test).

second messengers might explain why agonists and antagonists of 5-HT$_6$R result in conflicting effects in different studies (Marazziti et al., 2011).

There are many functional interactions between signaling and membrane trafficking (Ponimaskin et al., 2005; Renner et al., 2012). The best example is β-arrestin, which binds to GPCRs and evokes their internalization through clathrin-coated pits but also functions to activate various signaling cascades (DeWire et al., 2007). Likewise, SNX14 modulates G-protein signaling as well as GPCR trafficking, suggesting that SNX14 bilaterally modulates Gαs-linked GPCRs signaling as a dual negative regulator. Although not examined in this study, Gαs is known to traffic through lipid rafts and its sequestration attenuates Gαs signaling (Allen et al., 2009). Participation of SNX14 in this process might add another level of regulation relevant to psychiatric disorders (Donati et al., 2008; Donati and Rasenick, 2003).

Although we have not investigated a possible role of SNX14 on receptor insertion or recycling, we believe that the role of SNX14 resides in the endocytic realm for the following reasons. First, when we treated with dynasore to block the endocytosis, we found that the levels of 5-HT$_6$R gradually increased even in the presence of SNX14 (supplementary material Fig. S4A). This suggested that SNX14 does not affect the insertion of the receptor. Second, a lysosomal inhibitor, chloroquine also induced a gradual increase of 5-HT$_6$R levels in the presence of SNX14 (supplementary material Fig. S4B), suggesting that SNX14 does not affect the recycling of the receptor.

Regulators of Gαs-linked GPCRs should have crucial roles in CNS, but specific RGS proteins for Gαs in the brain have yet to be found. Although the RGS domain of SNX13 is reported to function as a specific GAP for Gαs (Zheng et al., 2001), its expression is high in heart and skeletal muscles but virtually absent in brain. The RGS domain of axin is known to bind Gαs, but it also interacts $G\alpha_{12}$ or $G\alpha_o$, thus showing no specificity for Gαs (Castellone et al., 2005). SNX25 also contains an RGS domain and induces TGF-β receptor degradation or interacts with D_1, D_2 dopamine receptors playing a role in trafficking. Our

Journal of Cell Science (2015) 128, 1848–1861 doi:10.1242/jcs.169581

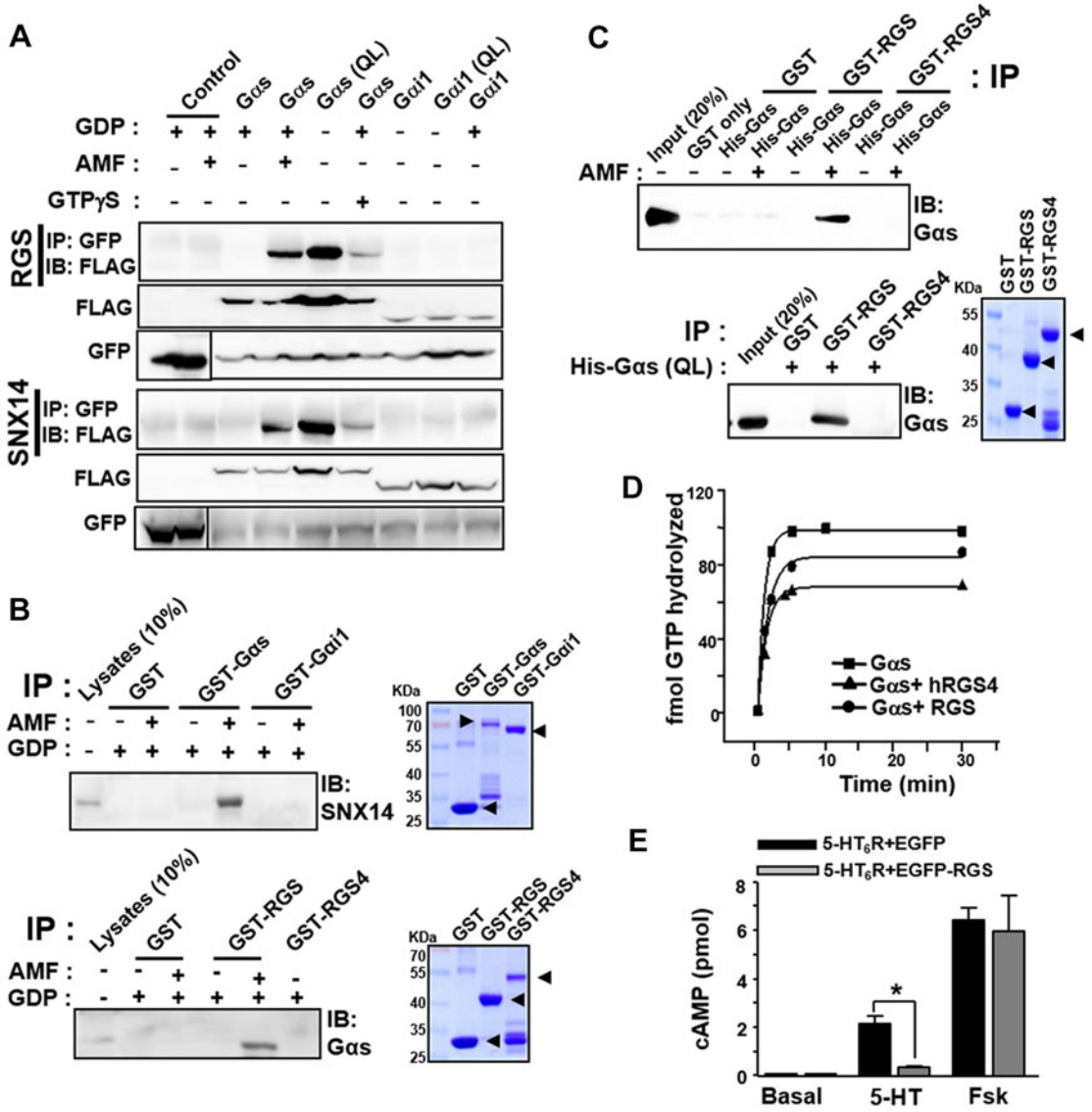

Fig. 5. SNX14 contains a non-functional RGS domain and specifically binds and sequesters Gαs, thus inhibiting 5-HT$_6$R-induced cAMP production. (A) HEK293T cells were co-transfected with an EGFP-tagged RGS domain of SNX14 (EGFP–RGS, amino acids 336–468) or EGFP–SNX14 and FLAG-tagged Gαs (wild-type, WT), Gαs with a Q227L mutation (QL, at residue 227), Gαi1 (WT) or Gαi1 with a Q204L mutation (QL, residue 204). 48 h after transfection, the cells were lysed and immunoprecipitated (IP) with anti-GFP antibody and immunoblotted (IB) with anti-FLAG antibody in the presence or absence of AMF, GDP or GTPγS. GFP lanes are shown separated due to different protein size. (B) Purified GST, GST-tagged Gαs, Gαi1, the RGS domain from SNX14 (GST–RGS) or RGS4 (10 μg) glutathione–agarose beads were incubated overnight at 4°C in the presence or absence of AMF with 10 mg of mouse brain lysate containing 100 μM GDP. Right panel, Coomassie-stained SDS-PAGE gels loaded with purified GST and GST fusion proteins used in the pulldown assay. (C) GST, GST–RGS or GST–RGS4 on glutathione–agarose beads (5 μg) were incubated with purified His–Gαs or His–Gαs (QL) in the presence or absence of GDP and/or AMF. Samples were immunoblotted with anti-Gαs antibody. Right panels, Coomassie-stained SDS-PAGE gels loaded with purified GST and GST fusion proteins used in the pulldown assay. (D) Quantitative detection of GAP activity of the SNX14 RGS domain and human RGS4 (hRGS4). Purified His–Gαs, GST–RGS of SNX14 and GST–hRGS4 were used for GTP hydrolysis assay. Gαs (closed squares, 90 nM) was assayed with RGS (closed circle, 900 nM) or hRGS4 (closed triangle, 500 nM). Neither RGS nor hRGS4 increased the rate of GTP hydrolysis of Gαs. (E) The RGS domain inhibits cAMP production induced by 5-HT treatment but not by forskolin (Fsk) treatment. HEK293T cells were co-transfected with 5-HT$_6$R and EGFP or EGFP–RGS and production of cAMP was measured. The data are means±s.e.m. from three independent experiments. *P<0.05 (paired t-test).

results show that SNX14 contains a RGS domain specific for Gαs. Despite its inability to act as a RGS-GAP, we demonstrated that SNX14 successfully inhibits the production of cAMP, thus we proposed that although it is not a classical GAP for Gαs, SNX14 acts as a negative regulator that inhibits Gαs-mediated downstream signaling pathways by binding and sequestering Gαs.

Regulation of RGS function by feedback phosphorylation is seen in other RGS or RGS-like proteins. Phosphorylation of RGS2 by protein kinase C (PKC) reduces its GAP activity (Cunningham et al., 2001) and ERK-mediated phosphorylation of RGS-GAIP increases its GAP activity (Ogier-Denis et al., 2000). Through phosphorylation, signaling cascades can be fine-tuned in either a feedback or feed-forward manner. The binding affinity of SNX14 for Gαs is dramatically decreased by PKA-mediated phosphorylation of its RGS domain; thereby relieving Gαs inhibition by SNX14 and facilitating Gαs activation of adenylyl

Journal of Cell Science (2015) 128, 1848–1861 doi:10.1242/jcs.169581

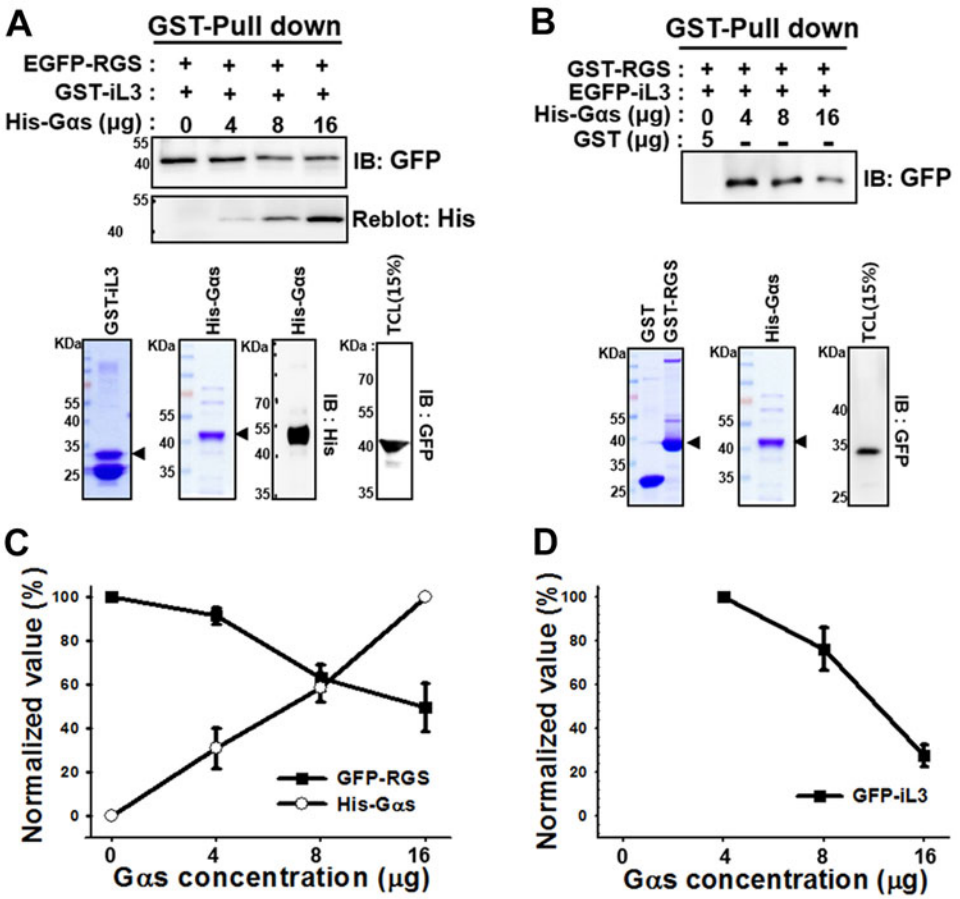

Fig. 6. The RGS domain of SNX14 and Gαs competitively bind to iL3 of 5-HT$_6$R. Purified GST-iL3 of 5-HT$_6$R was incubated with cell lysates (500 μg) from cells overexpressing the EGFP-tagged RGS domain of SNX14 (EGFP–RGS) and the indicated amounts of purified His–Gαs, and a GST pulldown assay was performed. The samples were immunoblotted with anti-GFP antibody, stripped and re-immunoblotted with anti-His antibody. Lower panels, Coomassie stains of 5 μg of GST-iL3, 2 μg of His-Gαs and immunoblots (IB) with anti-His antibody and anti-GFP antibody using 15% of the total cells lysate (TCL) as inputs. (B) 500 μg cell lysates from cells overexpressing EGFP-iL3 was pulled down with a purified SNX14 RGS domain (GST–RGS) and the indicated amount of purified His–Gαs. Samples were immunoblotted with anti-GFP antibody. The interaction between RGS and iL3 was substantially decreased with the increased amount of Gαs. A Coomassie staining of purified GST (5 μg), GST–RGS (10 μg) and His–Gαs (2 μg) is also shown. 15% of the TCL was loaded as inputs. (C,D) Quantification from three independent experiments as described in A and D, respectively. Data were normalized to the maximum intensity of each protein.

cyclase and the subsequent cAMP signaling pathways. Thus, activation of the 5-HT$_6$R-mediated cAMP–PKA pathway depends on the extent of SNX14 phosphorylation by PKA, suggesting that this might fine-tune 5-HT$_6$R-mediated signaling in the brain which might contribute to the cellular responses observed in neurological and psychiatric disorders, suggesting SNX14 as a potential therapeutic target.

MATERIALS AND METHODS

DNA constructs

The full-length of mouse SNX14 was amplified by PCR from an Image cDNA clone (Invitrogen, Carlsbad, CA) and subcloned into pEGFP-C1 (Clontech, Palo Alto, CA) and pGEX-4T-1 (Amersham Biosciences, Arlington Hts, IL). The PXA-RGS-PX domain (amino acids 130–937), the RGS-PX domain (amino acids 336–937), the PXA domain (amino acids 130–304), the RGS domain (amino acids 336–468) and the PX domain (amino acids 558–937) of SNX14 were subcloned into EGFP or mCherry empty vector. 6×His-RGSPX was cloned into pcDNA-3.1A (Invitrogen, San Diego, CA). HA-tagged β_2AR, Gαs (WT), Gαs (Q227L), Gαi1 (WT) and Gαi1 (Q204L) were cloned into pCMV4-FLAG vector (Sigma, St. Louis, MO). HA–β_2AR, HA-RGS4 and 3×HA-5-HT$_6$R were purchased from the Missouri S&T cDNA Resource Center (Rolla, MO). PM-GFP was constructed by subcloning of the GAP-43 membrane anchoring domain into pDisplay-EGFP vector (Invitrogen). The fidelity of all constructs was verified by DNA sequencing.

Antibodies

The anti-SNX14 antibody was raised against RAENTERKQNQNY (amino acids 759–771) and anti-human SNX14 polyclonal antibody was purchased from Sigma. Other antibodies used were: anti-GFP (EMD Millipore, Billerica, MA), anti-His (QIAGEN, Valencia, CA), anti-transferrin receptor, anti-EEA1 (BD Biosciences, San Jose, CA), anti-β-actin, anti-β-tubulin, anti-β-tubulin-III, anti-phosphoserine, anti-phosphothreonine, anti-phosphotyrosine (EMD Millipore), anti-FLAG, anti-GST (Sigma), anti-5-HT$_6$R (H-143; Santa Cruz Biotechnology, Santa Cruz, CA), anti-rat HA (Roche, Basel, Switzerland), anti-mouse HA (COVANCE, Princeton, CA), anti-Gαs (Santa Cruz Biotechnology) and secondary antibodies conjugated to Alexa Fluor 405, 488 or 594 (Invitrogen).

Protein-lipid overlay assay

Protein–lipid overlay assays were performed using PIP strips (Echelon Research Laboratories, Salt Lake City, UT). Membranes were blocked with 3% (w/v) BSA in Tris-buffered saline with 0.1% Tween 20 (TBS-T) for 1 h at room temperature. Membranes were incubated overnight at 4℃ in 3% BSA/TBS-T, together with 0.5 μg/ml of various purified GST-tagged proteins. Membranes were further incubated with anti-GST antibody for 1 h at room temperature, probed with horseradish peroxide (HRP)-conjugated anti-rabbit IgG antibody (Jackson ImmunoResearch, West Grove, PA) and visualized by enhanced chemiluminescence (GE Healthcare Bio-Sciences, Uppsala, Sweden).

Tissue preparation and immunohistochemistry

Experiments were performed in accordance with guidelines set forth by the Seoul National University Council Directive for the proper care and use of laboratory animals. Mice were perfused transcardially with heparinized PBS followed by ice-cold 4% paraformaldehyde in PBS. Brains were removed, immersed in the same fixative for 4 h, cryoprotected by infiltration with 10–30% sucrose solution, embedded in an Optimal Cutting Temperature compound and rapidly frozen in 2-methanol. Specimens were cut into 35-μm coronal sections on a cryostat and immunostained with anti-SNX14 antibody. Sections were treated with 1% FBS with 0.3% Triton X-100 in PBS for 30 min, blocked with 1% H_2O_2 in PBS, rinsed with PBS, incubated with the primary antibody for overnight at

Journal of Cell Science (2015) 128, 1848–1861 doi:10.1242/jcs.169581

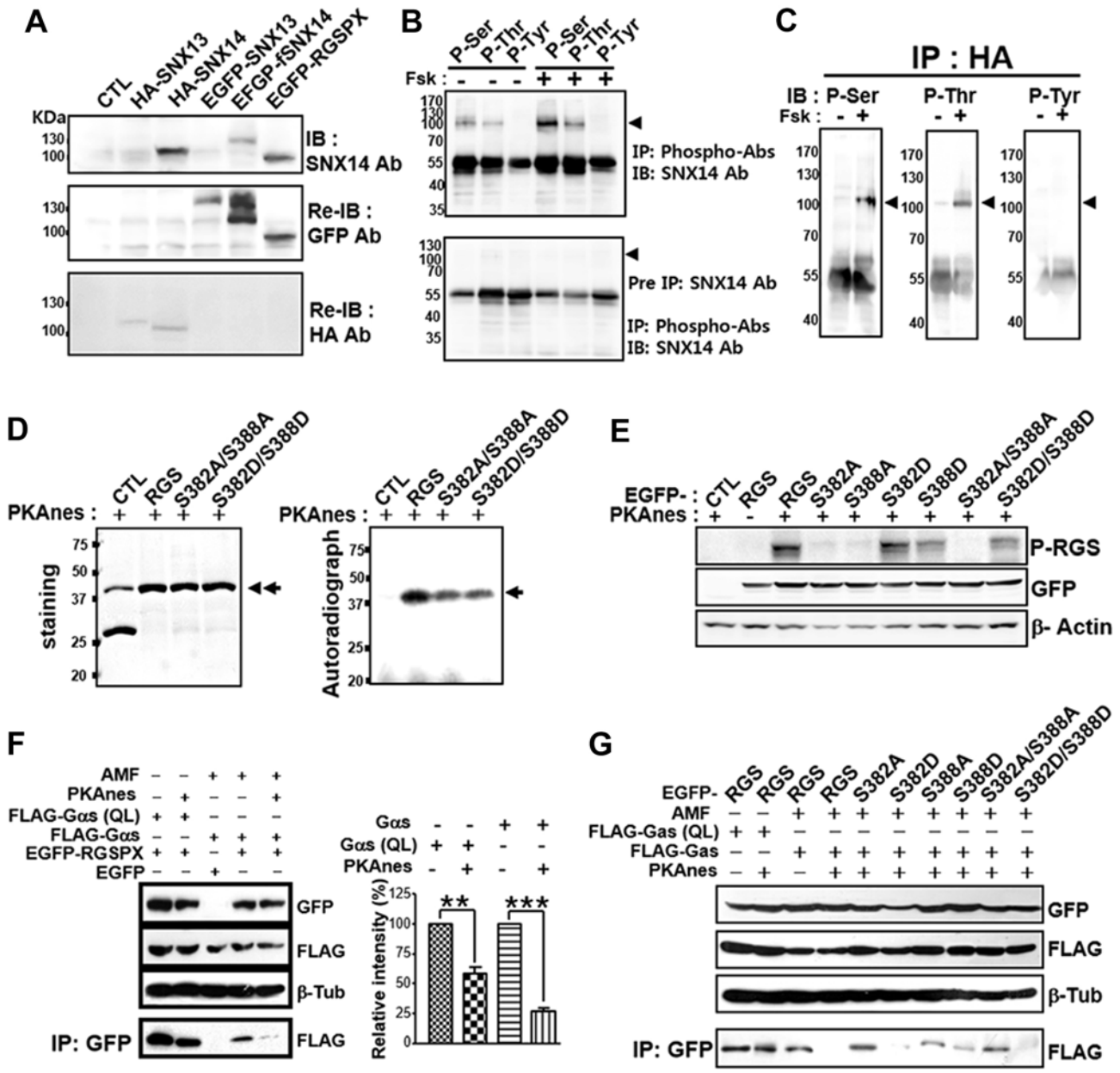

Fig. 7. See next page for legend.

4℃ and exposed to the HRP-conjugated anti-rabbit IgG (Rockland Immunochemicals, Gilbertsville, PA) for 1 h at room temperature. Immunostaining was visualized by staining with diaminobenzidine (Vector, Burlingame, CA) for 3 to 5 min and viewing under a FSX100 microscope (Olympus, Tokyo, Japan).

Cyclic AMP enzyme immunoassay

HEK293T cells were transfected using Lipofectamine-2000 (Invitrogen). At 48 h after transfection, the cells were starved for 16 h and treated with chemicals followed by 10 µM 5-HT for 20 min or 25 µM forskolin for 3 min. The cells were lysed and cAMP was measured with a cAMP direct immunoassay kit (Abcam, Cambridge, MA).

Single turnover GTPase assay

BL21 bacterial cells were transformed with GST–RGS, GST–RGS mutants (S382D/S388D and S382A/S388A), 6×His-Gαs and 6×His-Gαi1. In the case of Gαs, 90 nM protein was applied with 900 nM of either RGS or RGS mutants (S382D/S388D and S382A/S388A) or 500 nM human RGS proteins whereas 80 nM Gαi1 protein was used for assay. G proteins were loaded with [^{32}P]GTP and GTPase assays were carried out as described previously except that the assay temperature was 4℃ (Berman et al., 1996).

Immunoprecipitation and immunoblotting

HEK293T cells were co-transfected with 3×HA-5-HT$_6$R and various SNX14 mutants, lysed in a lysis buffer (20 mM Tris-HCl pH 8, 10% glycerol, 137 mM NaCl, 2 mM EDTA), and centrifuged for 20 min at 14,000 ***g*** at 4℃. 500 µg total proteins from the supernatant were incubated with anti-GFP, anti-FLAG, anti-phosphoserine, anti-phosphothreonine or anti-phosphotyrosine antibody overnight at 4℃, incubated with 30 µl of protein-A–Sepharose for 1 h, pelleted by centrifugation and analyzed by SDS-PAGE. Proteins on the gels were transferred onto PVDF membranes (Pall Life Sciences, Ann Arbor, MI) and incubated with primary antibodies for 1 h at room temperature. The

Fig. 7. PKA phosphorylates SNX14 at Ser 382 and Ser 388 and re-routes SNX14 from Gαs to 5-HT$_6$R, facilitating internalization and degradation of that receptor. (A) HEK293T cells were transfected with EGFP (CTL), HA–SNX13, HA–SNX14, EGFP–SNX13, EGFP–SNX14 and EGFP–RGSPX. The cells were lysed and immunoblotted (IB) with anti-SNX14 antibody. Note that anti-SNX14 antibody does not recognize SNX13. Re-IB indicates membrane was stripped and re-probed with anti-GFP or anti-HA antibody to verify the expression of each protein. (B) HEK293T cells were transfected with HA–SNX14 and treated with or without 25 μM forskolin. Cells were lysed and immunoprecipitated (IP) with anti-phosphoserine (P-Ser), anti-phosphothreonine (P-Thr), or anti phosphotyrosine (P-Tyr) antibody, followed by immunoblotting with anti-SNX14 antibody (upper panel). Each arrowhead indicates SNX14. The same samples were preincubated with anti-SNX14 antibody and were immunoprecipitated with protein-A beads. The supernatants were incubated with anti-phospho-antibodies as indicated and immunoblotted with anti-SNX14 antibody (lower panel). Each arrowhead indicates SNX14. Given that preincubation with anti-SNX14 antibody removes all SNX14 from the supernatant, no band was detected, again confirming the specificity of anti-SNX14 antibody. (C) HEK293T cells were transfected with HA–SNX14 and treated with or without 25 μM forskolin. The cells were lysed and immunoprecipitated with anti-HA antibody, followed by immunoblotting with anti-phospho-antibodies. Note that SNX14 was phosphorylated by forskolin on serine and threonine residues but not on tyrosine residues. (D) Phosphorylation of the RGS domain of SNX14 by PKA *in vitro*. Purified GST (CTL) or GST-fusion proteins [wild-type, phospho-deficient (S382A/S388A) and phospho-mimetic (S382D/S388D) mutants] were incubated with a purified catalytic subunit of PKA at 30˚C for 2 h in kinase buffer with [γ-^{32}P]ATP. The proteins were resolved by SDS-PAGE and detected by autoradiography (right panel) and by staining with Coomassie Brilliant Blue (left panel). The arrow indicates RGS proteins and the arrowhead indicates a PKA catalytic subunit. (E) HEK293T cells were co-transfected with EGFP (CTL) or EGFP-tagged wild-type, various phospho-deficient (S382A, S388A) or phospho-mimetic (S382D, S388D) mutants and PKAnes (PKA catalytic subunit). The cells were lysed and immunoprecipitated with anti-GFP antibody, immunoblotted with anti-phosphoserine antibody. P-RGS, phosphorylated RGS. (F) Cells were co-transfected with EGFP, the EGFP-tagged RGS-PX domain of SNX14 (EGFP–RGSPX) and/or FLAG-Gαs (WT), FLAG-Gαs QL (Q227L) and PKAnes. After 48 h transfection, the cells were treated with or without AMF, lysed, immunoprecipitated with anti-GFP antibody and immunoblotted with anti-FLAG antibody. The interaction between Gαs (WT or Q227L) and SNX14 was diminished by PKAnes. Net intensity of immunoblotted Gαs (WT or Q227L) was normalized to the value of Gαs (WT or Q227L) in the absence of PKAnes. Data are the mean±s.e.m. (n=5). **P<0.01; ***P<0.001 (paired t-test). (G) Phosphorylation of the RGS domain blocks Gαs association and RGS phospho-mimetics also fail to bind Gαs. HEK293T cells were cotransfected with FLAG-tagged Gαs (WT) or Gαs (Q227L) and the EGFP-tagged RGS domain of SNX14 (EGFP–RGS), various phospho-deficient or phospho-mimetic RGS domain mutants and PKAnes in the presence or absence of AMF. The cells were lysed, immunoprecipitated with anti-GFP antibody followed by immunoblotting with anti-FLAG antibody. Phosphorylation of RGS proteins by co-transfection of PKAnes inhibits the interaction between the RGS and Gαs WT or Gαs Q227L (first four lanes). Phospho-mimetic mutants lost the ability to interact with Gαs, even in the presence of AMF (last six lanes).

immunoreactions were detected with SuperSignal West Pico Chemiluminescent Substrate (Thermo Scientific, Rockford, IL).

Cell culture, transfection and immunocytochemistry

HEK293T, COS-7 and HT-22 cells were cultured at 37˚C and 5% CO_2 in Dulbecco's Modified Eagle's Medium (DMEM, Invitrogen) supplemented with 10% FBS (Hyclone, Logan, UT) and transfected using Lipofectamine-2000. Fluorescence images were acquired on an Olympus IX-71 microscope (Olympus) using a CoolSNAP-HQ camera (Roper Scientific, Tucson, AZ) driven by MetaMorph software (Molecular Devices, Sunnyvale, CA). The confocal images were acquired on an Olympus FV-1000 confocal microscope with 100×, 1.4 NA oil-immersion objective lens. For immunocytochemistry, cells were fixed in 4% formaldehyde and 4% sucrose in PBS for 15 min, permeabilized for 5 min in 0.25% Triton X-100 in PBS and blocked for 30 min in 10% BSA in PBS at 37˚C. The cells were incubated with primary antibodies for 2 h and secondary antibodies for 45 min at 37˚C in 3% BSA in PBS. For the colocalization assay, COS-7 cells were permeabilized with 0.05% saponin for 1 min at 4˚C before fixation. Analysis and quantification were performed with MetaMorph and SigmaPlot 8.0 (Systat Software, San Jose, CA).

TIRF microscopy

Cells were imaged using an Olympus IX-71 microscope fitted with a 60×, 1.45 NA TIRF-lens and controlled by Cell^M software (Olympus). 488 and 561 nm diode lasers were coupled to the TIRF microscopy condenser through two independent optical fibers. Using software, we changed the angle of the incident laser to get the calculated penetration depth of <120 nm. Cells were typically imaged either in single channel or in two channels by sequential excitation with 0.1-s exposures and detected with a Andor iXon 897 EMCCD camera (512×512; Andor Technologies, Belfast, Northern Ireland). The Image J program (National Institutes of Health) was used for analysis.

PKA kinase assay

GST-RGS of SNX14 (0.5 mg/ml) was incubated with 1000 units/ml catalytic subunit of PKA (New England Biolabs, Ipswich, MA) at 30˚C for 2 h in 50 mM Tris-HCl pH 7.5, 10 mM $MgCl_2$ and 200 μM ATP. For the autoradiography, the reaction mixture was supplemented with γ-labeled ATP to a final specific activity of 200 μCi/μmol. RGS phosphorylation was assayed in the presence of reducing agents.

Surface biotinylation and membrane protein extraction

3×HA-5-HT$_6$R stable cells were transfected with various SNX14 mutants. 48 h after transfection, cells were starved for 16 h in serum-free media and treated with 10 μM 5-HT for the times indicated. The cells were washed with ice-cold PBS, incubated with 0.25 mg/ml EZ-Link® Sulfo-NHS-SS-Biotin in PBS for 30 min at 4˚C, rinsed in Quenching Solution with TBS to remove free biotin reagents, and lysed. After centrifugation, the supernatants were incubated with 50 μl of 50% slurry of immobilized NeutraAvidin for 2 h at 4˚C. To detect internalized 5-HT$_6$R (Fig. 3D,E), 3×HA-5-HT$_6$R stable cells were transfected with various SNX14 mutants. After starvation, surface proteins were biotinylated with 0.25 mg/ml EZ-Link® Sulfo-NHS-SS-Biotin in PBS for 30 min at 4˚C. Unreacted biotin was removed by 50 mM glycine in PBS for 10 min at 4˚C and washed with cold PBS. The cells were treated with 10 μM 5-HT for indicated times and washed with cold PBS. Non-endocytosed biotin was cleaved in 50 mM glutathione, 75 mM NaCl and 75 mM NaOH in FBS solution for 20 min at 4˚C. After blocking and washing, cells were lysed and immunoprecipitated with NeutraAvidin for 2 h at 4˚C. Biotinylated proteins were eluted in SDS sample buffer followed by immunoblotting with an anti-HA antibody.

In-gel digestion and MS sample preparation

Immunoprecipitated protein samples were separated by one-dimensional SDS-PAGE and protein bands of interest were excised from the gel for an in-gel digestion procedure. Tryptic digest peptides obtained from the in-gel digestion procedure were dissolved in 0.1% formic acid and 5% acetonitrile solution for mass spectrometry analysis.

Dephosphorylation by alkaline phosphatase treatment

Tryptic digest peptide samples obtained from the in-gel digestion procedure were also resuspended in 1×NEBuffer-3 and alkaline phosphatase solution (10 unit/μl) was added to remove phosphate moieties. After incubation for 2 h at 37˚C, the dephosphorylation was stopped by adding formic acid solution to a final concentration of 5%.

Micro-LC-MS/MS analysis

In-gel digested peptide samples and alkaline phosphatase-treated peptide samples were subjected to micro-LC-MS/MS experiments using an LTQ ion trap mass spectrometer (ThermoElectron, San Jose, CA). Details of the micro LC-MS/MS analysis and protein database search process are as

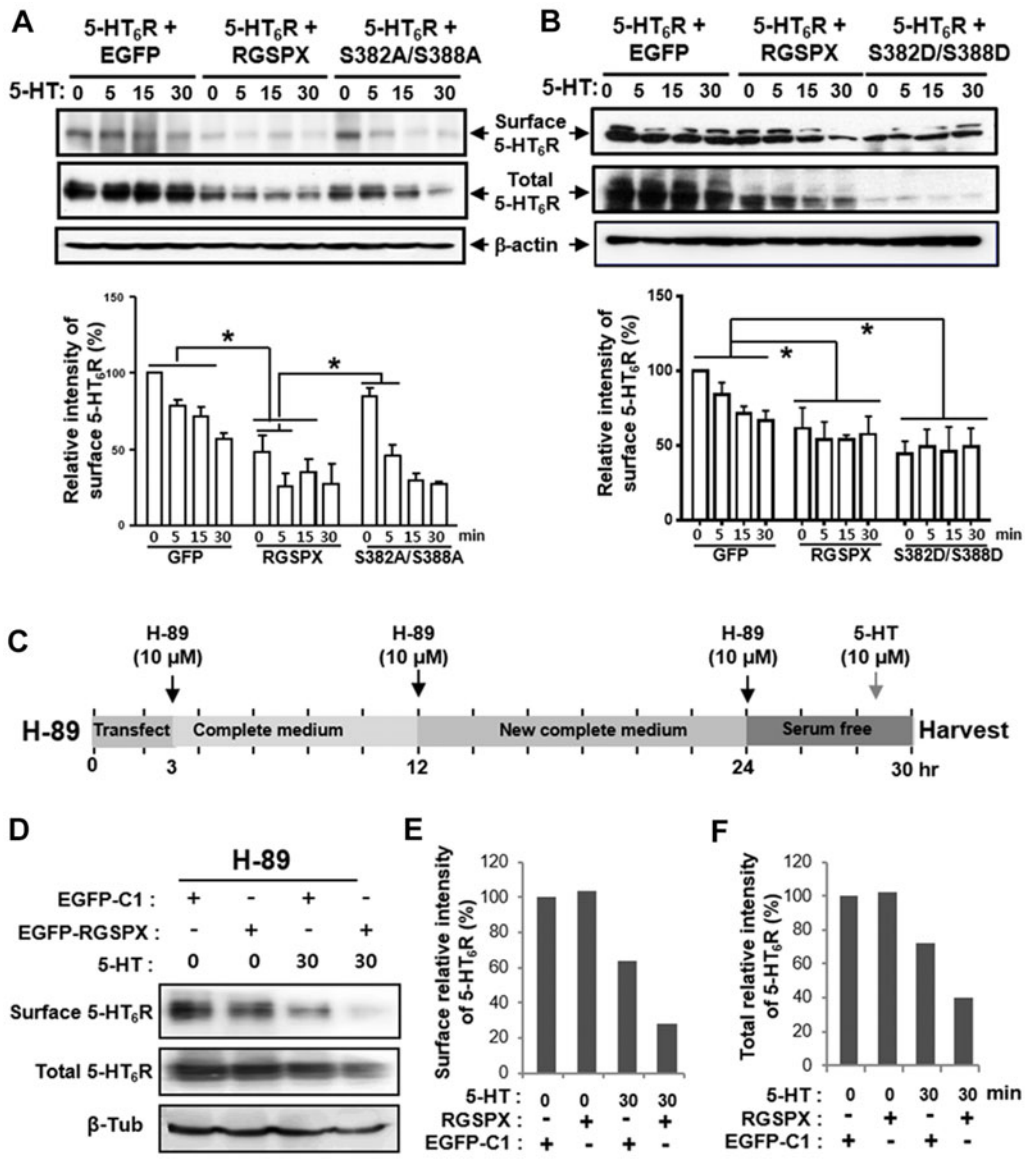

Fig. 8. Phosphorylation of SNX14 affects the SNX14-induced internalization of surface 5-HT$_6$R. (A,B) Phosphorylation of SNX14 is required for the initial reduction of 5-HT$_6$R. HEK293T cells were co-transfected with HA–5-HT$_6$R and EGFP-C1 (control), the EGFP-tagged RGS-PX domain of SNX14 (EGFP–RGSPX), and EGFP-phospho-deficient (S382A/S388A) or EGFP-phospho-mimetic RGS-PX domain mutants (S382D/S388D). The cells were starved for 5.5 h and incubated with 10 μM 5-HT for the times indicated, then surface biotinylation was performed. All of the quantitation assays were carried out in triplicate and the results were normalized to the levels of EGFP group at time 0. Lower graphs, the quantification from three independent experiments. Asterisks indicate significant changes between the RGS-PX domain group and EGFP group and between the S382A/S388A group and the RGS-PX domain group at matching time points. *P<0.05 (ANOVA and Tukey's HSD post hoc test). (C) Experimental scheme of PKA inhibitor (H-89) treatment. HEK293 cells stably expressing 5-HT$_6$R were transfected with EGFP-C1 or EGFP–RGSPX. 10 μM H-89 was added into culture medium as indicated in the scheme. The total and surface proteins were extracted 30 h after transfection. (D) Immunoblotting was performed with anti-HA and anti-β-tubulin antibodies after treatment as described in C. SNX14 affects neither the initial levels of total nor that of surface 5-HT$_6$R. (E,F) Quantification of surface (E) or total (F) 5-HT$_6$R levels after 5-HT treatment in the presence or absence of H-89. The surface or total levels of 5-HT$_6$R was normalized to that at time 0 after 5-HT treatment.

described elsewhere (Choi et al., 2011). Briefly, peptides were separated by C18 reversed phase capillary column and Agilent HP1100 quaternary LC pump. Solvent A (3% HCOOH, 5% CH_3CN and 92% H_2O) and Solvent B (3% HCOOH, 5% CH_3CN and 92% H_2O) were used to make a 120-min gradient. MS/MS spectra obtained in the micro-LC-MS/MS analysis were searched against an in-house protein database containing both SNX14 and EGFP using Bioworks Ver.3.2 and Sequest Cluster System. The differential modification search options for phosphorylation modification (+80 on Ser, Thr, Tyr) and oxidation (+16 on Met) were considered in the search and the maximum number of modifications that were allowed per peptide was seven. Manual assignments of fragment ions in each MS/MS spectrum were performed to confirm the database search results.

RNA interference

The small hairpin RNAs (shRNAs) from three nucleotides 42–52 (shRNA-1), 183–189 (shRNA-2), and 536–542 (shRNA-3) of the mouse SNX14 cDNA sequence (NM_172926) were designed. A pair of complementary oligonucleotides was synthesized separately with the addition of an ApaI site at the 5′-end and an *Eco*RI site at the 3′-end. The forward primer sequences were 5′-CAGGTATCTGCATGTCTTATT-CAAGAGATAAGACATGCAGATACCTGTTTT-3′, 5′-GGTGGATA-

TTCCATCTATTTTCAAGAGAAATAGATGGAATATCCACCTTTT-3′ and 5′-GAGGATGACTCTCCAGTAGTTCAAGAGACTACTGGA-GAGTCATCCTCTTTT-3′ (the underlined letters are the SNX14-siRNA sequences). The annealed cDNA fragment was cloned into the *Apa*I-*Eco*RI sites of pSilencer-1.0-U6-mRFP vector (Ambion, Austin, TX). The knockdown efficiency was tested in the HT-22 cells and EGFP–SNX14-transfected HEK293T cells.

Protein delivery

The cloned 6×His-RGSPX in pET-23b vector (EMD Millipore) was transformed into BL-21 and cultured in 2×YT medium supplemented with ampicillin. After overnight induction with 0.5 mM IPTG at 30℃, cells were sonicated in the lysis buffer (50 mM NaH_2PO_4 pH 8.0, 300 mM NaCl, 5 mM Decyl-β-D-Maltopyranoside (Anatrace, Maumee, OH) and centrifuged for 60 min at 13,000 ***g***. The supernatants were incubated with Ni-NTA agarose (Qiagen) at 4℃ for 30 min. The beads were then washed extensively with lysis buffer and the protein was eluted with an elution buffer (50 mM NaH_2PO_4 pH 8.0, 200 mM NaCl, 200 mM imidazole). To further purify 6×His-RGSPX, whole proteins were filtered with an Ultracel-30K centrifugal filter (Millipore, Billerica, MA) at 5000 ***g*** for 10 min and the supernatant was immediately applied to a Superdex 200 10/300 GL column (GE Healthcare) at a flow rate of 0.5 ml/min at 4℃. Proteins were collected by a FPLC-NGC chromatography system. The purified 6×His-RGSPX protein was introduced to 5-HT_6R stable HEK293 cells using Chariot (Active Motif, Carlsbad, CA). Briefly, 4 µl of Chariot was diluted in 40 µl of 80% DMSO, mixed with 40 µl of PBS containing purified the RGS-PX domain (1.25 µg) and followed by 30 min incubation at room temperature. The complex was diluted in serum-free DMEM to a volume of 200 µl and added to 5-HT_6R stable cells. The cells were incubated with the complexes in serum-free medium for 1 h, followed by 1 ml serum-containing medium for 2 h.

Acknowledgements

We thank Jung-Ah Kim for critical reading of the manuscript. Confocal and TIRF microscopy data were acquired in the Biomedical Imaging Center.

Competing interests

The authors declare no competing or financial interests.

Author contributions

C.H.M., M.M.R. and S.C. designed the study. C.H.M., D.P., Y.K., M.N., S.P., S.W., H.K. and H.R. performed experiments and data analysis. C.H.M., D.P., H.K., H.R., Z.Y.P. and S.C. interpreted experimental results. C.H.M., D.P., Z.Y.P., M.M.R. and S.C. wrote the manuscript. All authors approved the final manuscript.

Funding

This research was supported by grants from the National Research Foundation (NRF) of Korea [grant numbers SRC 20100029395 and 20100029395 to S.C.]; by the Education and Research Encouragement Fund of Seoul National University Hospital to S.C.; by the Basic Science Research Program [grant number 2010-0022375]; and KBRI research program [grant numbers 20140006 and 20150002 to C.M.H.]. This research also supported by the US Public Health Service [grant number MH07800] and the US Veteran's Administration [grant number BX001149] to M.M.R.

Supplementary material

Supplementary material available online at
http://jcs.biologists.org/lookup/suppl/doi:10.1242/jcs.169581/-/DC1

References

Allen, J. A., Yu, J. Z., Dave, R. H., Bhatnagar, A., Roth, B. L. and Rasenick, M. M. (2009). Caveolin-1 and lipid microdomains regulate Gs trafficking and attenuate Gs/adenylyl cyclase signaling. *Mol. Pharmacol.* **76**, 1082-1093.

Berman, D. M., Wilkie, T. M. and Gilman, A. G. (1996). GAIP and RGS4 are GTPase-activating proteins for the Gi subfamily of G protein alpha subunits. *Cell* **86**, 445-452.

Castellone, M. D., Teramoto, H., Williams, B. O., Druey, K. M. and Gutkind, J. S. (2005). Prostaglandin E2 promotes colon cancer cell growth through a Gs-axin-beta-catenin signaling axis. *Science* **310**, 1504-1510.

Carlton, J., Bujny, M., Rutherford, A. and Cullen, P. (2005). Sorting nexins-unifying trends and new perspectives. *Traffic.* **6**, 75-82.

Carroll, P., Renoncourt, Y., Gayet, O., De Bovis, B. and Alonso, S. (2001). Sorting nexin-14, a gene expressed in motoneurons trapped by an in vitro preselection method. *Dev. Dyn.* **221**, 431-442.

Choi, H., Lee, S., Jun, C. D. and Park, Z. Y. (2011). Development of an off-line capillary column IMAC phosphopeptide enrichment method for label-free phosphorylation relative quantification. *J. Chromatogr. B Analyt. Technol. Biomed. Life Sci.* **879**, 2991-2997.

Cunningham, M. L., Waldo, G. L., Hollinger, S., Hepler, J. R. and Harden, T. K. (2001). Protein kinase C phosphorylates RGS2 and modulates its capacity for negative regulation of Galpha 11 signaling. *J. Biol. Chem.* **276**, 5438-5444.

Dawson, L. A. (2011). The central role of 5-HT6 receptors in modulating brain neurochemistry. *Int. Rev. Neurobiol.* **96**, 1-26.

De Vries, L., Zheng, B., Fischer, T., Elenko, E. and Farquhar, M. G. (2000). The regulator of G protein signaling family. *Annu. Rev. Pharmacol. Toxicol.* **40**, 235-271.

DeWire, S. M., Ahn, S., Lefkowitz, R. J. and Shenoy, S. K. (2007). Beta-arrestins and cell signaling. *Annu. Rev. Physiol.* **69**, 483-510.

Donati, R. J., Dwivedi, Y., Roberts, R. C., Conley, R. R., Pandey, G. N. and Rasenick, M. M. (2008). Postmortem brain tissue of depressed suicides reveals increased Gs alpha localization in lipid raft domains where it is less likely to activate adenylyl cyclase *J. Neurosci.* **28**, 3042-3050.

Donati, R. J. and Rasenick, M. M. (2003). G protein signaling and the molecular basis of antidepressant action. *Life Sci.* **73**, 1-17.

Duhr, F., Déléris, P., Raynaud, F., Séveno, M., Morisset-Lopez, S., Mannoury la Cour, C., Millan, M. J., Bockaert, J., Marin, P. and Chaumont-Dubel, S. (2014). Cdk5 induces constitutive activation of 5-HT6 receptors to promote neurite growth. *Nat. Chem. Biol.* **10**, 590-597.

Geldenhuys, W. J. and Van der Schyf, C. J. (2008). Serotonin 5-HT6 receptor antagonists for the treatment of Alzheimer's disease. *Curr. Top. Med. Chem.* **8**, 1035-1048.

Heal, D., Gosden, J. and Smith, S. (2011). The 5-HT6 receptor as a target for developing novel antiobesity drugs. *Int. Rev. Neurobiol.* **96**, 73-109.

Hill, S. J. (2006). G-protein-coupled receptors: past, present and future. *Br. J. Pharmacol.* **147 Suppl. 1**, S27-S37.

Huang, H. S., Yoon, B. J., Brooks, S., Bakal, R., Berrios, J., Larsen, R. S., Wallace, M. L., Han, J. E., Chung, E. H., Zylka, M. J. et al. (2014). Snx14 regulates neuronal excitability, promotes synaptic transmission, and is imprinted in the brain of mice. *PLoS ONE* **9**, e98383.

Kang, H., Lee, W. K., Choi, Y. H., Vukoti, K. M., Bang, W. G. and Yu, Y. G. (2005). Molecular analysis of the interaction between the intracellular loops of the human serotonin receptor type 6 (5-HT6) and the alpha subunit of GS protein. *Biochem. Biophys. Res. Commun.* **329**, 684-692.

Kim, S. H., Kim, D. H., Lee, K. H., Im, S. K., Hur, E. M., Chung, K. C. and Rhim, H. (2014). Direct interaction and functional coupling between human 5-HT6 receptor and the light chain 1 subunit of the microtubule-associated protein 1B (MAP1B-LC1). *PLoS ONE* **9**, e91402.

Lecca, D., Piras, G., Driscoll, P., Giorgi, O. and Corda, M. G. (2004). A differential activation of dopamine output in the shell and core of the nucleus accumbens is associated with the motor responses to addictive drugs: a brain dialysis study in Roman high- and low-avoidance rats. *Neuropharmacology* **46**, 688-699.

Marazziti, D., Baroni, S., Catena Dell'Osso, M., Bordi, F. and Borsini, F. (2011). Serotonin receptors of type 6 (5-HT6): what can we expect from them? *Curr. Med. Chem.* **18**, 2783-2790.

Marcos, B., Aisa, B. and Ramírez, M. J. (2008). Functional interaction between 5-HT(6) receptors and hypothalamic-pituitary-adrenal axis: cognitive implications. *Neuropharmacology* **54**, 708-714.

Masellis, M., Basile, V. S., Meltzer, H. Y., Lieberman, J. A., Sevy, S., Goldman, D. A., Hamblin, M. W., Macciardi, F. M. and Kennedy, J. L. (2001). Lack of association between the T—>C 267 serotonin 5-HT6 receptor gene (HTR6) polymorphism and prediction of response to clozapine in schizophrenia. *Schizophr. Res.* **47**, 49-58.

Meffre, J., Chaumont-Dubel, S., Mannoury la Cour, C., Loiseau, F., Watson, D. J., Dekeyne, A., Séveno, M., Rivet, J. M., Gaven, F., Déléris, P. et al. (2012). 5-HT(6) receptor recruitment of mTOR as a mechanism for perturbed cognition in schizophrenia. *EMBO Mol. Med.* **4**, 1043-1056.

Milligan, G. and Kostenis, E. (2006). Heterotrimeric G-proteins: a short history. *Br. J. Pharmacol.* **147 Suppl. 1**, S46-S55.

Mitchell, E. S. and Neumaier, J. F. (2005). 5-HT6 receptors: a novel target for cognitive enhancement. *Pharmacol. Ther.* **108**, 320-333.

Mitchell, E. S., Sexton, T. and Neumaier, J. F. (2007). Increased expression of 5-HT6 receptors in the rat dorsomedial striatum impairs instrumental learning. *Neuropsychopharmacology* **32**, 1520-1530.

Monsma, F. J., Jr, Shen, Y., Ward, R. P., Hamblin, M. W. and Sibley, D. R. (1993). Cloning and expression of a novel serotonin receptor with high affinity for tricyclic psychotropic drugs. *Mol. Pharmacol.* **43**, 320-327.

Neubig, R. R. and Siderovski, D. P. (2002). Regulators of G-protein signalling as new central nervous system drug targets. *Nat. Rev. Drug Discov.* **1**, 187-197.

Ogier-Denis, E., Pattingre, S., El Benna, J. and Codogno, P. (2000). Erk1/2-dependent phosphorylation of Galpha-interacting protein stimulates its GTPase accelerating activity and autophagy in human colon cancer cells. *J. Biol. Chem.* **275**, 39090-39095.

Ponimaskin, E., Dumuis, A., Gaven, F., Barthet, G., Heine, M., Glebov, K., Richter, D. W. and Oppermann, M. (2005). Palmitoylation of the 5-hydroxytryptamine4a

receptor regulates receptor phosphorylation, desensitization, and beta-arrestin-mediated endocytosis. *Mol. Pharmacol.* **67**, 1434-1443.

Renner, U., Zeug, A., Woehler, A., Niebert, M., Dityatev, A., Dityateva, G., Gorinski, N., Guseva, D., Abdel-Galil, D., Fröhlich, M. et al. (2012). Heterodimerization of serotonin receptors 5-HT1A and 5-HT7 differentially regulates receptor signalling and trafficking. *J. Cell Sci.* **125**, 2486-2499.

Ruat, M., Traiffort, E., Arrang, J. M., Tardivel-Lacombe, J., Diaz, J., Leurs, R. and Schwartz, J. C. (1993). A novel rat serotonin (5-HT6) receptor: molecular cloning, localization and stimulation of cAMP accumulation. *Biochem. Biophys. Res. Commun.* **193**, 268-276.

Svenningsson, P., Tzavara, E. T., Qi, H., Carruthers, R., Witkin, J. M., Nomikos, G. G. and Greengard, P. (2007). Biochemical and behavioral evidence for antidepressant-like effects of 5-HT6 receptor stimulation. *J. Neurosci.* **27**, 4201-4209.

Tesmer, J. J., Berman, D. M., Gilman, A. G. and Sprang, S. R. (1997). Structure of RGS4 bound to AlF4—activated G(i alpha1): stabilization of the transition state for GTP hydrolysis. *Cell* **89**, 251-261.

Thomas, A. C., Williams, H., Setó-Salvia, N., Bacchelli, C., Jenkins, D., O'Sullivan, M., Mengrelis, K., Ishida, M., Ocaka, L., Chanudet, E. et al. (2014). Mutations in SNX14 cause a distinctive autosomal-recessive cerebellar ataxia and intellectual disability syndrome. *Am. J. Hum. Genet.* **95**, 611-621.

Ward, R. P., Hamblin, M. W., Lachowicz, J. E., Hoffman, B. J., Sibley, D. R. and Dorsa, D. M. (1995). Localization of serotonin subtype 6 receptor messenger RNA in the rat brain by in situ hybridization histochemistry. *Neuroscience* **64**, 1105-1111.

Worby, C. A. and Dixon, J. E. (2002). Sorting out the cellular functions of sorting nexins. *Nat. Rev. Mol. Cell Biol.* **3**, 919-931.

Xu, Y., Hortsman, H., Seet, L., Wong, S. H. and Hong, W. (2001). SNX3 regulates endosomal function through its PX-domain-mediated interaction with PtdIns(3)P. *Nat. Cell Biol.* **3**, 658-666.

Yun, H. M., Kim, S., Kim, H. J., Kostenis, E., Kim, J. I., Seong, J. Y., Baik, J. H. and Rhim, H. (2007). The novel cellular mechanism of human 5-HT6 receptor through an interaction with Fyn. *J. Biol. Chem.* **282**, 5496-5505.

Yun, H. M., Baik, J. H., Kang, I., Jin, C. and Rhim, H. (2010). Physical interaction of Jab1 with human serotonin 6 G-protein-coupled receptor and their possible roles in cell survival. *J. Biol. Chem.* **285**, 10016-10029.

Zheng, B., Ma, Y. C., Ostrom, R. S., Lavoie, C., Gill, G. N., Insel, P. A., Huang, X. Y. and Farquhar, M. G. (2001). RGS-PX1, a GAP for GalphaS and sorting nexin in vesicular trafficking. *Science* **294**, 1939-1942.

Supplemental Figure Legends

Supplemental Fig. 1. The alignment of other RGS proteins with the RGS domain of SNX14 and diverse phosphoinositide binding properties and cellular localizations of PX, PXA or full-length of SNX14. (A) Among all species, conserved residues are shaded in gray and identical residues in black. Asterisks indicate identical residues between SNX13 and SNX14 and diamonds indicate similar residues. (B) The expression of SNX14 protein increases gradually during neuronal development. The cells were prepared at the indicated days *in vitro* (DIV), lysed and loaded onto SDS-polyacrylamide gels. Western blot analysis was performed using antibodies as indicated. GFAP, glial fibrillary acidic protein; Tub, tubulin. (C) Protein-lipid overlay assay was performed using purified GST-PX, PXA and full-length SNX14, respectively. The PX domain strongly binds to PtdIns(3)P and PtdIns(5)P while the PXA domain binds to PtdIns(3,4)P_2, PtdIns(4,5)P_2 and PtdIns(3,4,5)P_3. (D) The subcellular localization of each deletion mutant or full-length of SNX14. COS-7 cells were transfected with EGFP-tagged SNX14 or its deletion mutants, then the subcellular localization of each group was observed with confocal microscope. The putative 2-transmembrane (2TM) (a.a. 1-75) was expressed in the endoplasmic reticulum. The PXA (a.a. 130-304) was expressed in the endosome-like structures and the RGS (a.a. 336-468) was mostly expressed in the cytosol and nucleus. The PX (a.a. 558-681), RGSPX (a.a. 336-397) and PXA-RGS-PX (a.a. 130-937) were expressed in the endosome-like punctate structures. The 3D view of EGFP-SNX14 expression pattern showed that it was expressed in the endosome-like punctate structures. Scale bars, 20 μm.

Supplemental Fig. 2. SNX14 co-localizes with G*α*s in the early endosomes and recruits G*α*s to the plasma membrane, and they internalize together. (A) Endogenous SNX14 is

translocated to the plasma membrane by ligand binding to 5-HT$_6$R. HT-22 cells were transfected with PM-GFP (GFP-tagged GAP43 membrane anchoring domain). 36 h after transfection, cells were treated with 10 μM 5-HT for 5 min at 37^{o}C, fixed and incubated with a specific anti-SNX14 antibody for 2 h, followed by incubation with an Alexa 594-conjugated anti-rabbit antibody for 40 min to detect endogenous SNX14. Scale bars, 10 μm. (B) COS-7 cells were transfected with Gαs-GFP alone, mCherry-SNX14 alone (mCh-SNX14) and mCh-SNX14 together with Gαs-GFP. 36 h after transfection, cells were permeabilized with 0.05% saponin for 1 min at 4^{o}C before fixation to release the cytosolic proteins and facilitate the detection of membrane-associated pools of SNX14 and Gαs. Fixed cells were incubated with anti-EEA1 antibody for 1 h, followed by Alexa594, 488 or 405-conjugated anti-mouse antibody for 45 min as indicated. Scale bar, 10 μm. (C) COS-7 cells were transfected with GFP-SNX14. 36 h after transfection, cells were fixed in 4% PFA and permeabilized with 0.25% Triton X-100 for 5 min. After PBS washing, cells were incubated with anti-transferrin receptor antibody (1:500) overnight at 4^{o}C and then were incubated with Texas-Red conjugated secondary antibody (1:2,000) for 45 min at 37^{o}C. Scale bar, 10 μm; Inset, 2.5 μm; Enlarged, 10 μm. (D) Gαs-EGFP and mCherry-SNX14 were co-transfected into 5-HT$_6$R stable HEK 293 cells and time-lapse TIRF images were acquired every 5 s with 200 ms exposure. Although there was some variability in the spatiotemporal relationship between Gαs and SNX14, a SNX14 burst was observed to occur either just before or coincidently with the Gαs burst and disappear together, suggesting that SNX14 is transiently recruited to the plasma membrane and both Gαs and SNX14 are internalized together. Scale bar, 10 μm; Inset, 2.5 μm. (D1, D2) The normalized fluorescence intensity changes are depicted as a function of time of the SNX14 spot (red) and its corresponding Gαs spot (green) pointed by each arrowhead in A and B, respectively.

Supplemental Fig. 3. Mass spectrometric identification of phosphorylation sites in the RGS domain of SNX14. HEK 293T cells were co-transfected with EGFP-RGS of SNX14 and PKA catalytic subunit. The cells were lysed and the contents were immunoprecipitated with anti-GFP antibody. Micro LC-MS/ MS analysis was then carried out to locate the phosphorylation sites in the RGS domain. Proteins were affinity-purified with anti-GFP antibody and subsequently separated by SDS-PAGE; bands were excised and in-gel digested using trypsin. Peptides were extracted and were analyzed with a Thermo LTQ linear ion trap mass spectrometer. (A) MS/ MS spectrum matched to the trypticphosphopeptide, ILRPELSNDEMoxLS*LHEELQK and (B) MS/ MS spectrum matched to the trypticphosphopeptide, ILRPELS*NDEMoxLSLHEELQK. Manual validations of major fragment ions were used to confirm the database search results. Fragment ions are assigned as b (blue color) or y (red color) series ions. Dark colored partial sequences indicate fragment ions resulting from neutral losses of either phosphoric acid or sulfenic acid. A mass accuracy of ± 0.5 Da was used in the assignments. * denotes phosphorylation sites. ^{OX} denotes oxidized methionine. (C) Conserved residues in all species are represented by asterisks and similar residues are represented as dots. The serine phosphorylation sites (S382/ S388) in RGS are conserved in mammals (open box). Sequence comparison was carried out by Clustal W (EMBL-EBI software).

Supplemental Fig. 4. SNX14 enhances the degradation of 5-HT$_6$R via endosome-lysosome pathways. (A) 5-HT$_6$R stable HEK 293 cells were transfected with EGFP-C1 or EGFP-RGSPX. 36 h after transfection, cells were pretreated with or without 80 μM dynasore for 20 min before incubation with10 μM 5-HT. The cells were lysed and immunoblotted with anti-

HA antibody. (B) Following 4 h treatment with 100 μM chloroquine, the cells were incubated with 10 μM 5-HT, lysed and immunoblotted with anti-HA antibody.

Supplemental Fig. 1.

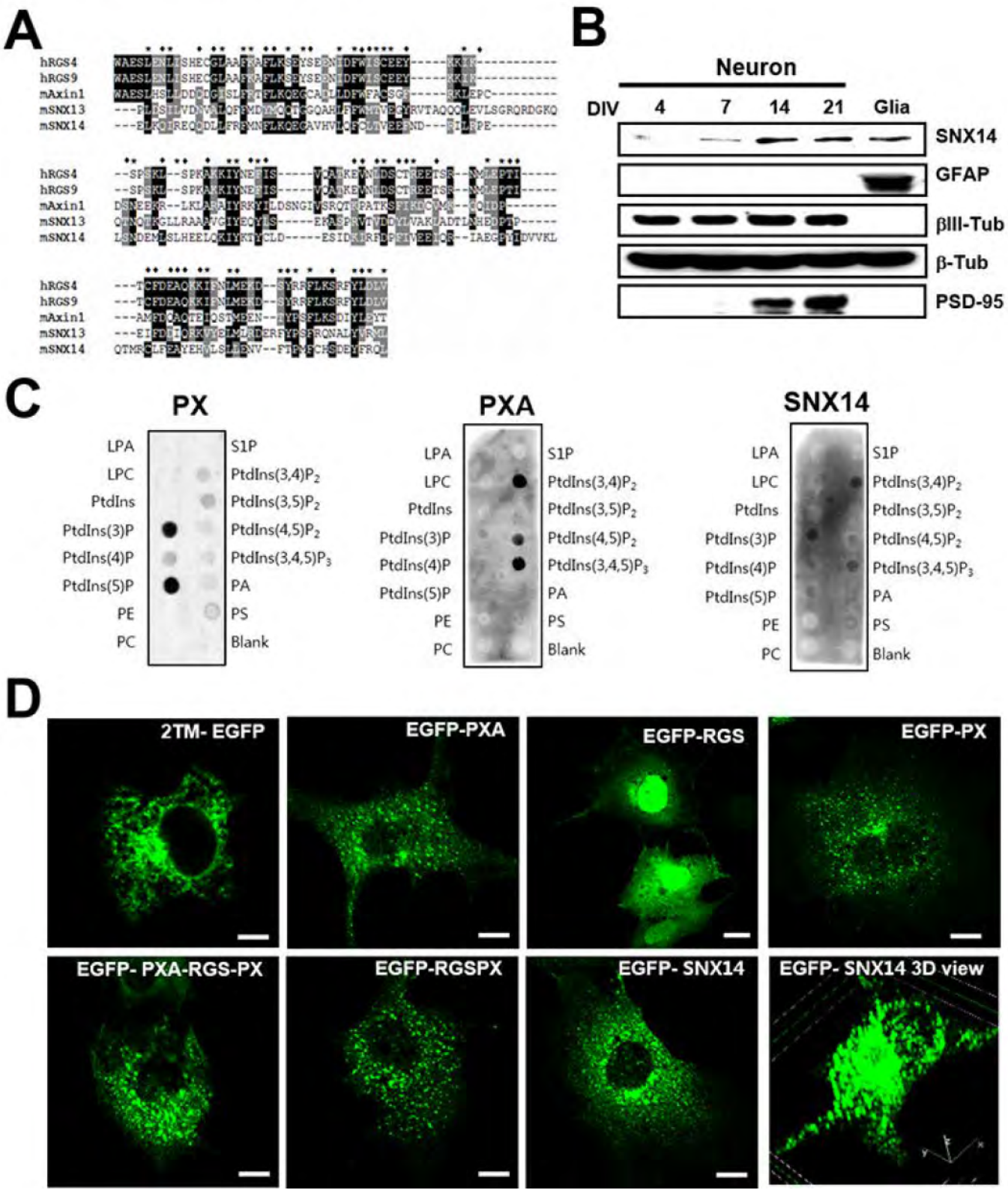

Supplemental Fig.2

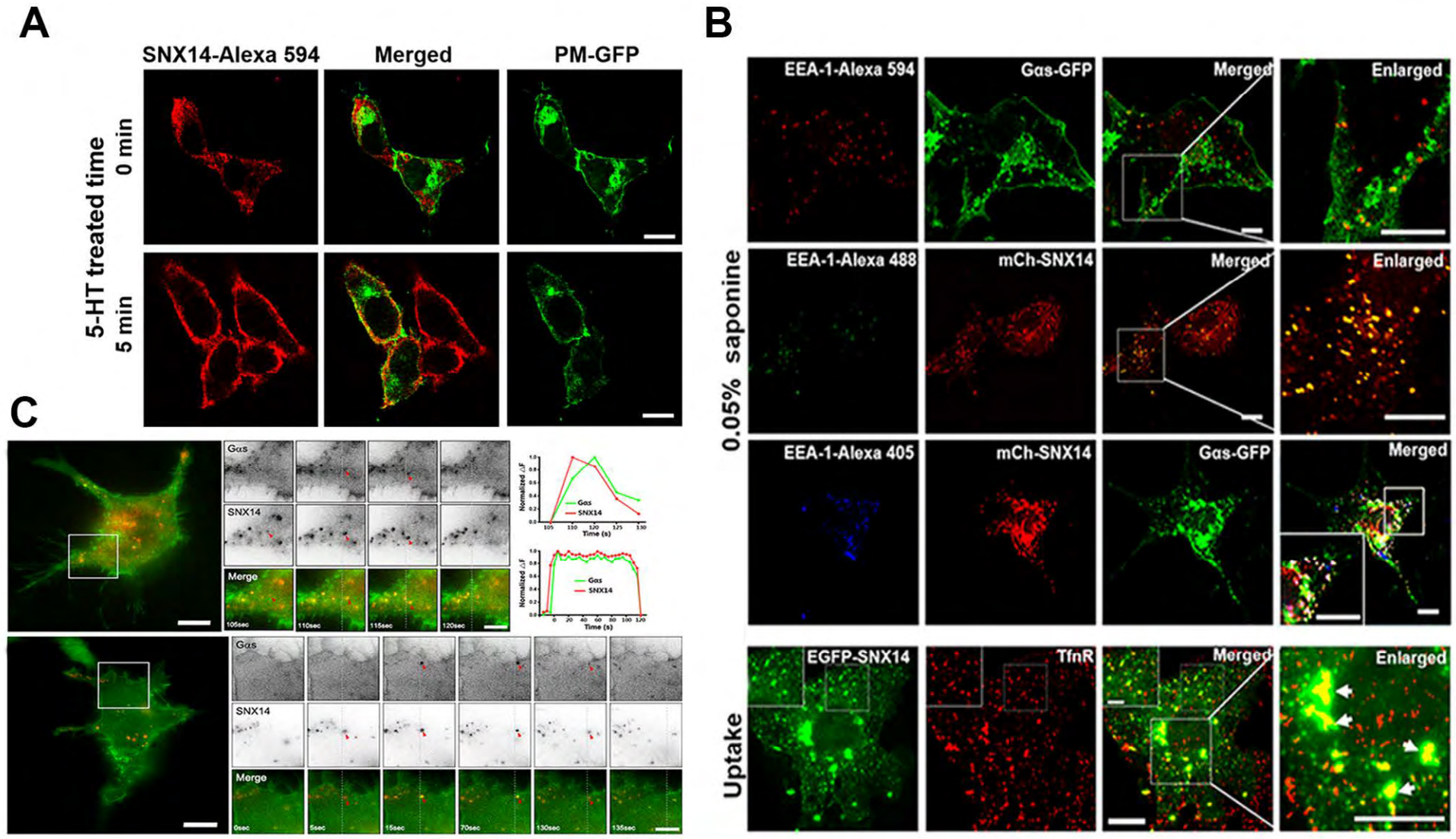

Supplemental Fig. 3.

A

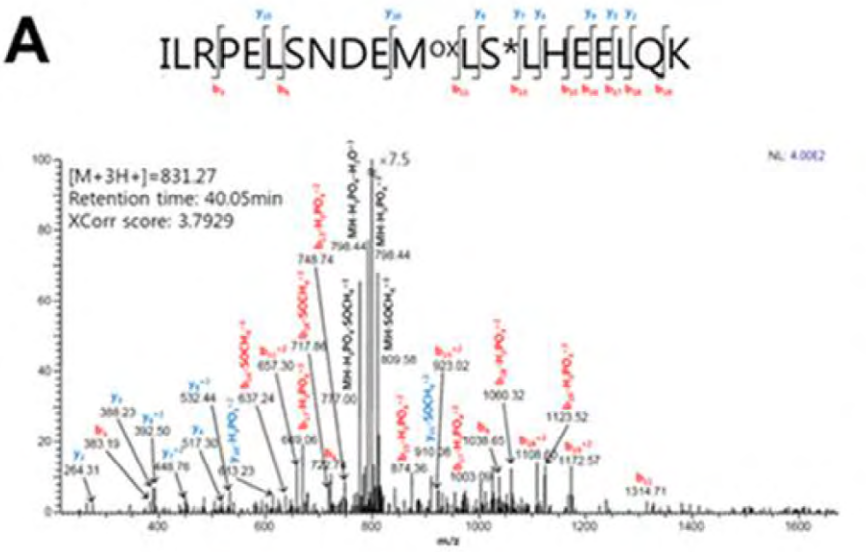

B

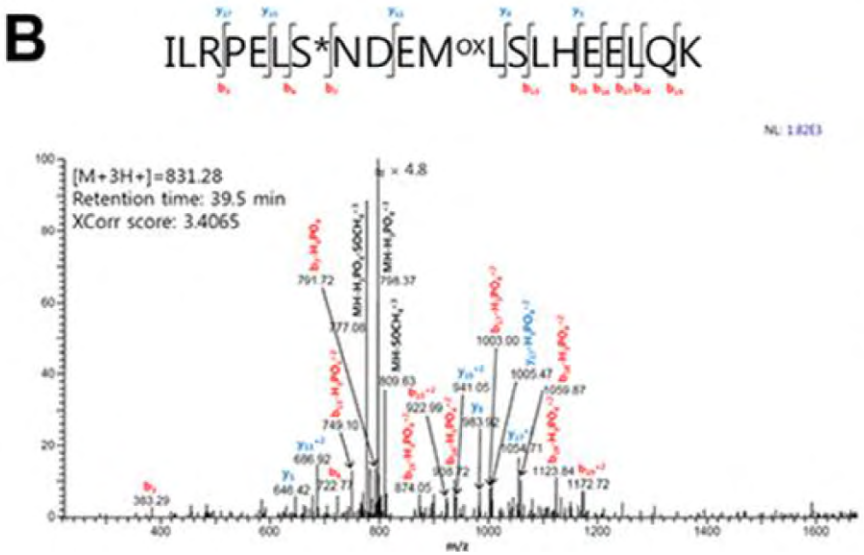

C

```
Mouse       ELKQIREQQDLLFRFMNFLKQE-GAVHVLQFCLTVEEFNDRILRPIISNDEMISLHEELQ 59
Human       ELKQIREQQDLLFRFMNFLKQE-GAVHVLQFCLTVEEFNDRILRPIISNDEMISLHEELQ 59
Chimpanzee  ELKQIREQQDLLFRFMNFLKQE-GAVHVLQFCLTVEEFNDRILRPIISNDEMISLHEELQ 59
Rat         ELKQIREQQDLLFRFMNFLKQE-GAVHVLQFCLTVEEFNDRILRPIISNDEMISLHEELQ 59
Dog         ELKQIREQQDLLFRFMNFLKQE-GAVHVLQICLTVEEFNDRILRPIISNDEMISLHEELQ 59
Chicken     ELKEIRDQQDLLFRFMNFLKQE-GAVHVLQFCLTVEEFNDRILRPIISDTEMIALHEEVQ 59
Frog        --------------FMNFLKQE-GAVHVLQFCLTVEEFNDKILRPIISDDELIALHKEVL 45
Worm        KLIEILRDARLYAIFRMYLQDIRGFVHELQFLVEAIRILDSIQRKLISDS---QIAYDIW 57
                          *  :*::  *.** **: : . .: * * *  *:    :  ::

Mouse       KIYKTYCLDESIDKIRFDPFIVEEIQRIAEGPYIDVVKLQTMRCLFEAYEHVLSLLENVF 119
Human       KIYKTYCLDESIDKIRFDPFIVEEIQRIAEGPYIDVVKLQTMRCLFEAYEHVLSLLENVF 119
Chimpanzee  KIYKTYCLDESIDKIRFDPFIVEEIQRIAEGPYIDVVKLQTMRCLFEAYEHVLSLLENVF 119
Rat         KIYKTYCLDESIDKIRFDPFIVEEIQRIAEGPYIDVVKLQTMRCLFEAYEHVLSLLENVF 119
Dog         KIYKTYCLDESIDKIRFDPFIVEEIQKIAEGPYIDVVKLQTMRCLFEAYEHVLSLLENVF 119
Chicken     KIYKTYCLDESIDKIRFDPFIVEEIQRIAEGPYEDVVKLQTMRCLFEAYEHVLSLLENVF 119
Frog        KIYKTYCLEESIDKIRFDPFIVEEIHKIAEGPYKEVVKLQTMCCLFEAYEHVLSLLENVF 105
Worm        QLYGQFVHESAQERVRIAESLVEQYKSAVEVNDIRVLEG----IIEMSYQEVYNRTQSTH 113
            ::*  :  :.: :::*:   :**: :  .*     *::      :  :*:.* .  :...

Mouse       IPMFCHSDEYFRQL 133
Human       IPMFCHSDEYFRQL 133
Chimpanzee  IPMFCHSDEYFRQL 133
Rat         IPMFCHSDEYFRQL 133
Dog         IPMFCHSDEYFRQL 133
Chicken     IPMFCHSDEYFRHL 133
Frog        IPMFCHSDEYFRQL 119
Worm        VVAFCQSECFLGHL 127
            .  **:*: :: :*
```

Supplemental Fig. 4.